Heterozygous variants of multidrug and toxin extrusions (MATE1 and MATE2-K) have little influence on the disposition of metformin in diabetic patients

Kana Toyama[a], Atsushi Yonezawa[a], Masahiro Tsuda[a], Satohiro Masuda[a], Ikuko Yano[a], Tomohiro Terada[a], Riyo Osawa[a], Toshiya Katsura[a], Masaya Hosokawa[b], Shimpei Fujimoto[b], Nobuya Inagaki[b] and Ken-Ichi Inui[a]

Multidrug and toxin extrusions (MATE1/SLC47A1 and MATE2-K/SLC47A2) play important roles in the renal excretion of metformin. We have previously identified the nonsynonymous *MATE* variants with functional defects at low allelic frequencies. The purpose of this study was to evaluate the effects of heterozygous *MATE* variants on the disposition of metformin in mice and humans. Pharmacokinetic parameters of metformin in *Mate1*(±) heterozygous mice were comparable with those in *Mate1*(+/+) wild-type mice. Among 48 Japanese diabetic patients, seven patients carried heterozygous *MATE* variant and no patient carried homozygous *MATE* variant. There was no significant difference in oral clearance of metformin with or without heterozygous *MATE* variants. In addition, creatinine clearance, but not heterozygous *MATE* variants, significantly improved the model fit of metformin clearance by statistical analysis using the nonlinear mixed-effects modeling program. In conclusion, heterozygous *MATE* variants could not influence the disposition of metformin in diabetic patients. *Pharmacogenetics and Genomics* 20:135–138 © 2010 Wolters Kluwer Health | Lippincott Williams & Wilkins.

Pharmacogenetics and Genomics 2010, 20:135–138

Keywords: creatinine clearance, H^+/organic cation antiporter, metformin, organic cation transporter, pharmacokinetics

[a]Department of Pharmacy, Faculty of Medicine, Kyoto University Hospital and [b]Department of Diabetes and Clinical Nutrition, Graduate School of Medicine, Kyoto University, Sakyo-ku, Kyoto, Japan

Correspondence to Professor Ken-ichi Inui, PhD, Department of Pharmacy, Kyoto University Hospital, Sakyo-ku, Kyoto 606-8507, Japan
Tel: +81 75 751 3577; fax: +81 75 751 4207;
e-mail: inui@kuhp.kyoto-u.ac.jp

Received 17 September 2009 Accepted 16 November 2009

Metformin is widely used for the treatment of hyperglycemia in patients with noninsulin-dependent diabetes mellitus. The major pharmacological action of metformin involves the suppression of gluconeogenesis in the liver. Lactic acidosis is a rare but serious adverse effect of metformin, which occurs predominantly in patients with renal insufficiency. Clinical pharmacokinetic studies revealed that metformin is mainly excreted into urine in an unchanged form without hepatic metabolism, and that the renal clearance of metformin is approximately five times higher than creatinine clearance (Ccr) [1], suggesting that renal tubular secretion is a major route of metformin elimination. In human proximal tubules, multidrug and toxin extrusion 1 (MATE1/SLC47A1) and a kidney-specific isoform MATE2-K/SLC47A2 are localized at the brush-border membranes, which were characterized as H^+/organic cation antiporters [2]. In rodents, Mate1, but not Mate2, is expressed in the kidney [2]. Metformin is a substrate for MATE1 and MATE2-K, as well as organic cation transporter 2 (OCT2/SLC22A2), which is localized at the basolateral membranes of the kidney [2,3]. The functional significance of MATE in the kidney was previously shown using *Mate1* knockout mice [4]. On the basis of these backgrounds and findings, MATE1 and MATE2-K could play key roles in metformin tubular secretion in humans.

Genetic variants in *MATE* genes are likely to be one of the factors for interindividual variability in metformin pharmacokinetics and pharmacodynamics. Recently, we and another group identified nonsynonymous single nucleotide polymorphisms (SNPs) in coding region of *MATE* genes, some of which reduced the transport activity [5,6]. In addition, Becker *et al.* [7] reported that rs2289669G > A SNP in the *MATE1* gene was associated with the glucose-lowering effect, but metformin pharmacokinetics was not evaluated. Tzvetkov *et al.* [8] demonstrated that there was no relationship between the same SNP and metformin pharmacokinetics. However, rs2289669G > A SNP in the *MATE1* gene was located in noncoding intron region and there was no information about the effect of this non-coding SNP on the transport activity. Therefore, it is not clear whether the functional reduced nonsynonymous *MATE* variants alter metformin disposition. The allelic frequencies of all *MATE* variants were quite low, in the range of 0.6–2.4% [5,6]. Homozygous variants with functional loss of transport activity decrease drug elimination in most

Supplemental digital content is available for this article. Direct URL citations appear in the printed text and are provided in the HTML and PDF versions of this article on the journal's Website (*www.pharmacogeneticsandgenomics.com*).

1744-6872 © 2010 Wolters Kluwer Health | Lippincott Williams & Wilkins

DOI: 10.1097/FPC.0b013e328335639f

cases. The effect of heterozygous variants, in contrast, depends on the transporters and the drugs. In the breast cancer resistance protein (*BCRP/ABCG2*) gene, heterozygous Q141K variant caused elevated oral bioavailability of its substrate [9]. These results suggested that information about the influence of heterozygous as well as homozygous *MATE* variants on metformin pharmacokinetics is required for its safe use in clinical situations. In this study, therefore, we focused on the effect of heterozygous nonsynonymous *MATE* variants on metformin disposition in diabetic patients.

Using *Mate1*(+/+) wild-type, *Mate1*(±) heterozygous and *Mate1*(−/−) homozygous mice, we first examined the pharmacokinetics of metformin (Supplemental methods, Supplemental digital content 1 *http://links.lww.com/FPC/A82*). High plasma concentration and low urinary excretion of metformin were observed in *Mate1*(−/−) mice compared with *Mate1*(+/+) mice, whereas there was no difference between *Mate1*(±) and *Mate1*(+/+) mice (Fig. 1a and b). In addition, several pharmacokinetic parameters in *Mate1*(±) mice were comparable with those in *Mate1*(+/+) mice (Supplemental Table 1, Supplemental digital content 2 *http://links.lww.com/FPC/A83*). Mate1 protein expression levels in these three genotype mice are shown in Fig. 1c. The transport of metformin by HEK293 cells expressing mouse Mate1, mouse Oct1 or mouse Oct2 was confirmed (Supplemental Fig. 1, Supplemental digital content 3 *http://links.lww.com/FPC/A84*). Based on these results, we hypothesized that the heterozygous *MATE* variants do not influence on the metformin clearance in humans as well as in mice.

To address the species difference in *MATE* genes, pharmacokinetic evaluation was also carried out in humans. Forty-eight Japanese patients with diabetes mellitus were enrolled into this study. Blood samples were obtained at 0, 4, and 9 h after metformin administration, followed by the determination of plasma concentrations and genotype for *MATE1*, *MATE2-K*, and *OCT2* genes (Supplemental methods, Supplemental digital content 1 *http://links.lww.com/FPC/A82*). The oral clearance (CL/F) of metformin in diabetic patients was estimated by the empirical Bayesian method with the nonlinear mixed-effects modeling program NONMEM using a basic model: $CL/F=\theta 1$. Two MATE1-G64D variant carriers, two MATE1-L125F variant carriers, and one MATE1-D328A variant carrier were found in this study. In the *MATE2-K* gene, the G211V variant was found in two patients. All *MATE* variant carriers were heterozygotes and included in the *MATE*-heterozygous variant group. The plasma concentration–time profile after an oral administration of metformin in *MATE*-heterozygous variant group was similar to that in *MATE*-reference group (Supplemental Fig. 2, Supplemental digital content 4 *http://links.lww.com/FPC/A85*). Patient

Fig. 1

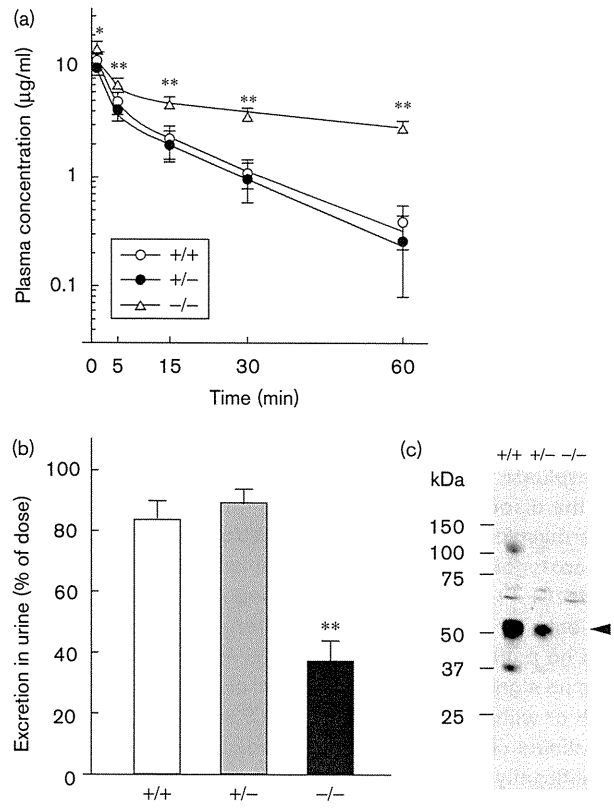

Metformin pharmacokinetic studies of *Mate1*(+/+), *Mate1*(±), and *Mate1*(−/−) mice. (a) Plasma concentration–time profiles were obtained after the intravenous administration of metformin to *Mate1* (+/+) (open circles), *Mate1*(±) (closed circles), and *Mate1*(−/−) (open triangles) mice. (b) Urinary excretion of metformin in *Mate1* (+/+) (open column), *Mate1*(±) (gray column), and *Mate1*(−/−) (closed column) mice were calculated using urine samples collected for 60 min after the drug administration. Each column represents the mean ± SD for six to eight mice. **P*<0.05, ***P*<0.01, significantly different from *Mate1*(+/+) mice. (c) Western blot analysis of Mate1 in renal brush-border membrane fractions was carried out. The arrowhead indicates the position of mouse Mate1.

characteristics were similar between the two groups. There was no statistically significant difference in metformin CL/F between the *MATE*-heterozygous variant group and the *MATE*-reference group (Table 1). All of 11 *OCT2* variant carriers were also heterozygotes. Only one patient carried both MATE1-G64D and OCT2-A270S variants. The CL/F values of the *MATE*-variant group, the *OCT2*-variant group and both the *MATE*-variant and *OCT2*-variant group were comparable with those of the reference group (Supplemental Table 2, Supplemental digital content 5 *http://links.lww.com/FPC/A86*).

To determine the most important factor contributing to interindividual variability in metformin CL/F, we examined the relationship between CL/F and patient characteristics, such as age, sex, renal function, and

Table 1 Patient characteristics and effects of heterozygous *MATE* variants on metformin oral clearance in 48 Japanese patients with diabetes mellitus

	MATE reference	MATE-heterozygous variant[a]
Patients	41	7
Sex (male/female)	17/24	1/6
Age (years)	62±10	67±8
BMI (kg/m^2)	27±4	25±3
Metformin CL/F (ml/min)	603±137	658±115
Ccr (ml/min)	98±34	83±37
eGFR (ml/min)	71±23	71±21

Ccr, 24-h creatinine clearance; CL/F, oral clearance of metformin; eGFR, estimated glomerular filtration rate; MATE, multidrug and toxin extrusion.
[a]*MATE*-heterozygous variant includes MATE1-G64D (n=2), MATE1-L125F (n=2), MATE1-D328A (n=1), MATE2-K-G211V (n=2). No patient carried other *MATE* variants; MATE1-V10L, MATE1-A310V, MATE1-V338I, MATE1-N474S, MATE1-V480M, MATE1-C497S, MATE1-Q519H, and MATE2-K-K64N. Data are expressed as mean±SD. There was no statistically significant difference between two groups.

transporter genetic variations. Regression analysis showed that metformin CL/F was positively correlated with both Ccr and estimated glomerular filtration rate (eGFR) (Supplemental Fig. 3, Supplemental digital content 6 *http://links.lww.com/FPC/A87*). In NONMEM analysis, model fit was significantly improved for the models using the individual Ccr or eGFR compared with the basic model (CL/F=θ1). However, there was no improvement in the models with age, sex or genetic variants of the *MATE* or *OCT2* gene. A negative of twice the log likelihood difference (−2LLD) value was higher in the model using Ccr than that using eGFR (Supplemental Table 3, Supplemental digital content 7 *http://links.lww.com/FPC/A88*). The incorporation of Ccr into the basic model explained part of the interindividual variability in CL/F, with its value decreasing from 26.1 to 19.6%.

Interindividual variability in MATE activity is likely to affect the pharmacokinetics of metformin. Examination with *Mate1* knockout mice strongly suggested the pharmacokinetic alternation in humans with the functional defect homozygous variants [4]. However, homozygous variants in *MATE1* and *MATE2-K* genes were reported to be quite rare [5,6]. Therefore, we examined the pharmacokinetic significance of the heterozygous *MATE* variants to clarify whether we should pay attention to these genotypes in the clinical situations. As expected from the animal data, the heterozygous *MATE* variants did not affect the disposition of metformin in humans (Fig. 1 and Table 1). The rate-limiting step in the renal secretion of metformin is either the renal blood flow, the tubular uptake across the basolateral membranes or efflux into the lumen at the brush-border membranes. In this study, heterozygous *MATE* variants did not affect metformin clearance, although MATE1 and MATE2-K were important for metformin secretion [2,3]. Likewise, heterozygous *OCT2* variant did not affect metformin clearance in diabetic patients, even though the pharmacokinetic effect of *OCT2* variant is still controversial [3,8,10]. The renal clearance of metformin was reported to be in the range of 335–615 ml/min in humans [1], which is comparable with renal plasma flow. These results suggested that renal blood flow is a rate-limiting factor for metformin secretion. Therefore, heterozygous *MATE* variants possibly show only a minor portion in the interindividual variation of metformin pharmacokinetics in clinical situations.

For determination of the most important factor contributing to metformin disposition among age, sex, renal function, and heterozygous variations of *MATE* and *OCT2* genes, NONMEM analysis was carried out. Consistent with previous reports [1,8], we showed that Ccr is a significant predictor of metformin clearance. Although Ccr is used clinically as a marker of GFR, Ccr is known to overestimate GFR because of the creatinine tubular secretion. Previously, we showed that creatinine is a substrate for OCT2, MATE1, and MATE2-K [2]. These reports suggested that creatinine as well as metformin is excreted into the urine by tubular secretion through organic cation transport systems in addition to glomerular filtration. Comparable with these findings, metformin CL/F had a higher correlation with Ccr than with eGFR. Therefore, Ccr is the most clinical reliable indicator of metformin disposition.

In conclusion, it was shown that heterozygous *MATE* variants as well as heterozygous *OCT2* variants do not affect metformin disposition in diabetic patients. Moreover, it was revealed that Ccr is the most important factor to predict metformin disposition in the clinical use. On account of the low allelic frequency, further studies are needed with much more patients to determine the effect of homozygous *MATE* variants on metformin disposition in clinical situations.

Acknowledgements

The authors are grateful to all the medical staff of Department of Diabetes and Clinical Nutrition, Graduate School of Medicine, Kyoto University, especially to Dr Chizumi Yamada, Dr Kazuyo Fujita, Dr Akio Obara, Dr Norio Harada, Dr Kazutaka Nagai, and Dr Shiho Takahara for excellent help. This study was supported in part by a grant-in-aid for Scientific Research (KAKENHI) from the Ministry of Education, Science, Culture, and Sports of Japan. M. Tsuda is a Research Fellow of the Japan Society for the Promotion of Science.

References

1 Scheen AJ. Clinical pharmacokinetics of metformin. *Clin Pharmacokinet* 1996; **30**:359–371.
2 Terada T, Inui K. Physiological and pharmacokinetic roles of H^+/organic cation antiporters (MATE/SLC47A). *Biochem Pharmacol* 2008; **75**:1689–1696.
3 Takane H, Shikata E, Otsubo K, Higuchi S, Ieiri I. Polymorphism in human organic cation transporters and metformin action. *Pharmacogenomics* 2008; **9**:415–422.

4 Tsuda M, Terada T, Mizuno T, Katsura T, Shimakura J, Inui K. Targeted disruption of the multidrug and toxin extrusion 1 (Mate1) gene in mice reduces renal secretion of metformin. *Mol Pharmacol* 2009; **75**:1280–1286.
5 Kajiwara M, Terada T, Ogasawara K, Iwano J, Katsura T, Fukatsu A, *et al.* Identification of multidrug and toxin extrusion (MATE1 and MATE2-K) variants with complete loss of transport activity. *J Hum Genet* 2009; **54**:40–46.
6 Chen Y, Teranishi K, Li S, Yee SW, Hesselson S, Stryke D, *et al.* Genetic variants in multidrug and toxic compound extrusion-1, hMATE1, alter transport function. *Pharmacogenomics J* 2009; **9**:127–136.
7 Becker MSL, Visser LE, van Schaik RHN, Hofman A, Uitterlinden AG, Stricker BHC. Genetic variation in the multidrug and toxin extrusion 1 transporter protein influences the glucose-lowering effect of metformin in patients with diabetes: a preliminary study. *Diabetes* 2009; **58**:745–749.
8 Tzvetkov MV, Vormfelde SV, Balen D, Meineke I, Schmidt T, Sehrt D, *et al.* The effects of genetic polymorphisms in the organic cation transporters OCT1, OCT2, and OCT3 on the renal clearance of metformin. *Clin Pharmacol Ther* 2009; **86**:299–306.
9 Sparreboom A, Gelderblom H, Marsh S, Ahluwalia R, Obach R, Principe P, *et al.* Diflomotecan pharmacokinetics in relation to ABCG2 421C>A genotype. *Clin Pharmacol Ther* 2004; **76**:38–44.
10 Chen Y, Li S, Brown C, Cheatham S, Castro RA, Leabman MK, *et al.* Effect of genetic variation in the organic cation transporter 2 on the renal elimination of metformin. *Pharmacogenet Genomics* 2009; **19**:497–504.

Rapamycin impairs metabolism-secretion coupling in rat pancreatic islets by suppressing carbohydrate metabolism

Makiko Shimodahira, Shimpei Fujimoto, Eri Mukai, Yasuhiko Nakamura, Yuichi Nishi, Mayumi Sasaki, Yuichi Sato, Hiroki Sato, Masaya Hosokawa, Kazuaki Nagashima, Yutaka Seino[1] and Nobuya Inagaki

Department of Diabetes and Clinical Nutrition, Graduate School of Medicine, Kyoto University, 54 Shogoin Kawahara-cho, Sakyo-ku, Kyoto 606-8507, Japan
[1]Kansai Electric Power Hospital, Osaka 553-0003, Japan
(Correspondence should be addressed to S Fujimoto; Email: fujimoto@metab.kuhp.kyoto-u.ac.jp)

Abstract

Rapamycin, an immunosuppressant used in human transplantation, impairs β-cell function, but the mechanism is unclear. Chronic (24 h) exposure to rapamycin concentration dependently suppressed 16·7 mM glucose-induced insulin release from islets (1·65±0·06, 30 nM rapamycin versus 2·35±0·11 ng/islet per 30 min, control, $n=30$, $P<0·01$) without affecting insulin and DNA contents. Rapamycin also decreased α-ketoisocaproate-induced insulin release, suggesting reduced mitochondrial carbohydrate metabolism. ATP content in the presence of 16·7 mM glucose was significantly reduced in rapamycin-treated islets (13·42 ±0·47, rapamycin versus 16·04±0·46 pmol/islet, control, $n=30$, $P<0·01$). Glucose oxidation, which indicates the velocity of metabolism in the Krebs cycle, was decreased by rapamycin in the presence of 16·7 mM glucose (30·1±2·7, rapamycin versus 42·2±3·3 pmol/islet per 90 min, control, $n=9$, $P<0·01$). Immunoblotting revealed that the expression of complex I, III, IV, and V was not affected by rapamycin. Mitochondrial ATP production indicated that the respiratory chain downstream of complex II was not affected, but that carbohydrate metabolism in the Krebs cycle was reduced by rapamycin. Analysis of enzymes in the Krebs cycle revealed that activity of α-ketoglutarate dehydrogenase (KGDH), which catalyzes one of the slowest reactions in the Krebs cycle, was reduced by rapamycin (10·08±0·82, rapamycin versus 13·82 ±0·84 nmol/mg mitochondrial protein per min, control, $n=5$, $P<0·01$). Considered together, these findings indicate that rapamycin suppresses high glucose-induced insulin secretion from pancreatic islets by reducing mitochondrial ATP production through suppression of carbohydrate metabolism in the Krebs cycle, together with reduced KGDH activity.
Journal of Endocrinology (2010) **204,** 37–46

Introduction

Rapamycin, an immunosuppressant used in human organ and tissue transplantation, exhibits a different mechanism of action from that of cyclosporine, tacrolimus, and corticosteroids. The agent is a macrolide that prevents T-cell activation through its inhibitory effect on serine/threonine kinase, the mechanistic target of rapamycin (MTOR). The insulin- and nutrient-signaling pathway through MTOR plays an important role in initiation of protein translation, a critical event in enhanced protein synthesis that leads to increased cell cycle progression and proliferation (McDaniel *et al.* 2002).

Brittle type 1 diabetes has been successfully treated by human islet transplantation using the Edmonton protocol, which includes use of rapamycin as an immunosuppressant (Shapiro *et al.* 2000). Some studies suggest rapamycin may be diabetogenic (Lu *et al.* 1994, Teutonico *et al.* 2005), and the effects of rapamycin on glucose homeostasis have been investigated. In skeletal muscle cells, long-term exposure to rapamycin decreases insulin-dependent uptake of glucose and glycogen synthesis and increases fatty acid oxidation (Sipula *et al.* 2006). Rapamycin also decreases insulin-mediated glucose uptake and insulin signaling in adipocytes (Taha *et al.* 1999, Cho *et al.* 2004). Interestingly, rapamycin both prevents β-cell mass expansion and impairs β-cell function (Bell *et al.* 2003, Zhang *et al.* 2006, Fraenkel *et al.* 2008).

In pancreatic β-cells, intracellular glucose metabolism regulates exocytosis of insulin granules according to metabolism-secretion coupling in which glucose-induced mitochondrial ATP production plays an essential role (Maechler & Wollheim 2001). Since depletion of mitochondrial DNA abolishes the glucose-induced ATP elevation, mitochondria clearly are a major source of ATP production in pancreatic β-cells (Kennedy *et al.* 1998, Tsuruzoe *et al.* 1998). Glucose-induced insulin secretion from β-cells is often impaired due to reduced glucose-induced ATP elevation by exposure to high concentrations of fuels including glucose, free fatty acids, and ketone body, and by administration of diabetogenic pharmacological agents (Fujimoto *et al.* 2007). Thus, reduced mitochondrial ATP production plays an important role in impaired glucose-induced insulin secretion.

Journal of Endocrinology (2010) **204,** 37–46
0022–0795/10/0204–037
DOI: 10.1677/JOE-09-0216
Online version via http://www.endocrinology-journals.org

Recently, several reports have shown that inhibition of MTOR by rapamycin decreases mitochondrial oxidative function using various materials including kidney mitochondria (Simon *et al.* 2003), Jurkat cells (Schieke *et al.* 2006), and skeletal tissue and cells (Cunningham *et al.* 2007). We investigated the effects of chronic exposure to rapamycin on metabolism-secretion coupling, especially on glucose metabolism in mitochondria, in pancreatic β-cells.

Materials and Methods

Materials

Rapamycin was purchased from Calbiochem (La Jolla, CA, USA). Disodium succinate, rotenone, pyruvate potassium, malate, and tetramethyl-*p*-phenyldiamine (TMPD) were purchased from Nacalai (Kyoto, Japan). Mouse monoclonal antibody to the subunits of the mitochondrial respiratory chain complex was obtained from Invitrogen. [5-^{3}H]-glucose, [U-^{14}C]-glucose, and anti-mouse IgG HRP-conjugated secondary antibody were obtained from GE Healthcare (Buckinghamshire, UK). Acetyl-CoA was obtained from Wako (Osaka, Japan). Luciferin–luciferase was obtained from Promega. All other reagents were obtained from Sigma Chemicals.

Animals

Male Wistar rats were obtained from Shimizu Co. (Kyoto, Japan). The animals were fed standard laboratory chow *ad libitum* and allowed free access to water in an air-conditioned room with a 12 h light:12 h darkness cycle until the experiments. All experiments were carried out with rats aged 8–11 weeks. The animals were maintained and used in accordance with the Guidelines for Animal Experiments of Kyoto University.

Islet isolation and culture

Islets of Langerhans were isolated from Wistar rats by collagenase digestion as previously described (Fujimoto *et al.* 1998). Isolated islets were cultured for 24 h in RPMI 1640 medium containing 10% FCS, 100 U/ml penicillin, 100 μg/ml streptomycin, and 5·5 mM glucose with or without rapamycin, at 37 °C in humidified air containing 5% CO_2.

Measurement of insulin release from isolated rat pancreatic islets, insulin content, and DNA content

Insulin release from intact islets was monitored using batch incubation as previously described (Fujimoto *et al.* 1998) using Krebs-Ringer bicarbonate buffer (KRBB) supplemented with 0·2% BSA (fraction V) and 10 mM HEPES adjusted to pH 7·4 (KRBB medium). After cultured islets were preincubated at 37 °C for 30 min in KRBB medium supplemented with 2·8 mM glucose, groups of five islets were batch incubated for 30 min in 0·7 ml KRBB medium containing 2·8 and 16·7 mM glucose with or without 100 μM α-tocopherol plus 200 μM ascorbate, or containing 2·8 and 16·7 mM α-ketoisocaproate (KIC). Before addition to KRBB medium, α-tocopherol was dissolved in ethanol at 1000-fold concentration. The same amount of ethanol was added to the control solution. At the end of the incubation period, the islets were pelleted by centrifugation, and aliquots of the buffer were sampled to determine the amount of immunoreactive insulin by RIA. After an aliquot of incubation medium for insulin release assay was taken, the islets remaining were lysed to determine insulin and DNA contents as previously described (Fujimoto *et al.* 2000).

Measurement of ATP content

ATP contents were determined as previously described (Kominato *et al.* 2008). Briefly, after groups of cultured islets were preincubated at 2·8 mM glucose for 30 min, groups of ten islets were incubated in tubes containing 0·5 ml KRBB medium supplemented with 2·8 or 16·7 mM glucose with or without 100 μM α-tocopherol plus 200 μM ascorbate at 37 °C for 30 min. Incubation was stopped by the addition of 0·1 ml of 2 M $HClO_4$. The contents of tubes were immediately mixed with vortex and sonicated in ice-cold water. The tubes were then centrifuged, and a fraction (0·4 ml) of the supernatant was mixed with 0·1 ml of 2 M HEPES and 0·1 ml of 1 M Na_2CO_3. The ATP concentration was measured by adding 0·2 ml luciferin–luciferase solution to a fraction sample (0·1 ml) in a bioluminometer (Luminometer Model 20e, Turner Designs, Sunnyvale, CA, USA). To draw a standard curve, blanks and ATP standards were run through the entire procedure including the extraction steps.

Measurement of glucose utilization and oxidation

Glucose utilization and oxidation were measured using the previously described method (Nabe *et al.* 2006). Briefly, cultured islets were preincubated in KRBB medium with 2·8 mM glucose at 37 °C for 30 min. For glucose utilization measurements, tubes containing 25 islets in 150 μl KRBB medium containing 2·8 or 16·7 mM glucose and 1·5 μCi [5-^{3}H] glucose were placed into glass vials containing 0·5 ml water. The capped vials were incubated at 37 °C for 90 min. After incubation was stopped by adding 50 μl of 1 M HCl into the incubation medium of the tubes without opening the caps, the capped vials were incubated overnight at 34 °C to allow $^{3}H_2O$ in the tubes to equilibrate with the water in the vial. Each tube was removed, and the disintegrations per minute of $^{3}H_2O$ in the water were counted. For oxidation measurements, procedures were the same as those for utilization measurements, except for the use of [U-^{14}C] glucose (0·5 μCi/tube) in place of [5-^{3}H] glucose and the use of 0·5 ml hydroxide of hyamine 10-X (Packard, Meriden, CT, USA) in place of 0·5 ml water.

Measurement of glucokinase activity

Glucokinase activity was measured by a fluorometric assay as previously described (Radu *et al.* 2005). Briefly, after cultured islets were preincubated with KRBB medium with 2·8 mM glucose, 100 islets were homogenized and the supernatants (islet extracts) were obtained from the homogenates by centrifugation. The glucose phosphorylation rate was estimated as the increase in NADH through the following reaction: glucose-6-phosphate + NAD^+ → 6-phosphoglucono-δ-lactone + NADH by NAD^+-dependent glucose-6-phosphate dehydrogenase (G6PDH). The enzyme reaction was performed using islet extracts in a solution containing NAD^+ and G6PDH supplemented with two concentrations (50 and 0·5 mM) of glucose at 37 °C for 1 h. NADH concentration was measured by fluorometry (Shimazu RF-5000, Kyoto, Japan). Glucokinase activity was determined by subtracting hexokinase activity measured at 0·5 mM glucose from the activity measured at 50 mM glucose.

Measurement of mitochondrial ATP production

Measurement of ATP production from mitochondrial fraction was performed as previously described (Takehiro *et al.* 2005). Briefly, to measure ATP production by oxidative phosphorylation, the reaction was started by adding mitochondrial suspension to prewarmed solution (37 °C) supplemented with the mitochondrial substrates, 50 μM ADP, and 1 μM diadenosine pentaphosphate (DAPP). DAPP is a specific inhibitor of adenylate kinase used to measure ATP production by oxidative phosphorylation exclusively. To normalize the mass of the intact mitochondria obtained, ATP production by adenylate kinase, one of the mitochondrial intermembrane kinases, was measured in the presence of ADP but without mitochondrial substrates or DAPP in parallel incubations. After reaction was stopped, the ATP concentration in the solutions was measured by adding luciferin–luciferase solution with a bioluminometer. ATP production was determined as the ratio of ATP production by oxidative phosphorylation to that by adenylate kinase.

Western blotting of mitochondrial respiratory chain complexes

After washing with ice-cold PBS, the cultured islets were solubilized in ice-cold lysis buffer (10 mM Tris (pH 7·2), 100 mM NaCl, 1 mM EDTA, 1% Nonidet P-40, and 0·5% sodium deoxycholate) containing protease inhibitor cocktail (Complete; Roche) with sonication (5 s pulse, five times). Protein content of the supernatant was measured and adjusted by Bradford method. The supernatant was dissolved in the same amount of SDS-PAGE sample buffer containing 100 mM Tris–HCl (pH 6·80), 4% SDS, 12% 2-mercaptoethanol, 20% glycerol, and 1% bromophenol blue and boiled for 5 min at 95 °C. The samples were subjected to electrophoresis on 12% SDS–polyacrylamide gels and transferred onto nitrocellulose membrane (Schleicher & Schuell, Keene, NH, USA). After blocking with TBS containing 0·1% Tween 20 and 5% skimmed milk (blocking buffer) for 1 h at 4 °C, blotted membranes were incubated overnight at 4 °C with mouse monoclonal anti-complex I (39 kDa subunit), anti-complex III (core II), anti-complex IV (subunit I), or anti-complex V (subunit α) of mitochondrial respiratory chain antibody at 1:1000 dilution in blocking buffer, and subsequently with anti-mouse IgG HRP-conjugated secondary antibody diluted 1:5000 at room temperature for 1 h prior to detection using ECL (GE Healthcare). In the same membrane, the process was repeated for β-actin at 1:5000 dilution of the antibody. Band intensities were quantified with Multi Gauge software (Fujifilm, Tokyo, Japan).

Measurement of activities of enzymes in Krebs cycle

Mitochondrial fraction obtained as described above was sonicated in ice-cold solution containing (mM) 180 KCl, 5 morpholinepropanesulfonic acid, and 2 EDTA adjusted to pH 7·40 and then diluted to each reaction mixture. Enzyme activities including NAD^+-linked isocitrate dehydrogenase (NAD-ICDH), aconitase, α-ketoglutarate dehydrogenase (KGDH), and malate dehydrogenase (MDH) were measured as previously described (Nulton-Persson & Szweda 2001). NAD-ICDH activities were measured as the rate of NAD^+ reduction in solution A containing (mM) 25 KH_2PO_4, 0·5 EDTA, and 0·01% Triton X-100 adjusted to pH 7·25 supplemented with 2·5 mM isocitrate, 40 μM rotenone, 5 mM $MgCl_2$, and 1 mM NAD^+. Aconitase activities were measured as the rate of $NADP^+$ reduction in solution A with 5 mM citrate, 0·6 mM $MgCl_2$, 1·0 U/ml NADP-ICDH, and 0·2 mM $NADP^+$. KGDH activities were measured as the rate of NAD^+ reduction in solution A with 2·5 mM α-ketoglutarate, 40 μM rotenone, 5·0 mM $MgCl_2$, 1 mM NAD^+, 0·1 mM CoA, and 0·2 mM thymine pyrophosphate (TPP). MDH activities were measured as the rate of NAD^+ reduction in solution A with 2·5 mM malate, 40 μM rotenone, 5 mM $MgCl_2$, 10 mM NAD^+, 0·3 mM acetyl-CoA, and 1 U/ml citrate synthase. Enzyme activities of pyruvate dehydrogenase (PDH) were measured as total PDH complex activity (Schwab *et al.* 2005) as the rate of *p*-iodonitrotetrazolium violet (INT) reduction in a reaction mixture containing 5 mM L-carnitine, 1·0 mM $MgCl_2$, 2·5 mM NAD^+, 0·1 mM CoA, 5 mM pyruvate, 0·2 mM TPP, 0·1% Triton X-100, 1 g/l BSA, 0·6 mM INT, and 6·5 mM phenazine methosulfate. All enzyme assays were performed at 25 °C.

Statistical analysis

The data are expressed as the mean ± S.E.M. Statistical significance was calculated by unpaired Student's *t*-test. $P<0·05$ was considered significant.

Results

Effect of chronic exposure to rapamycin on glucose-induced insulin release, insulin content, and DNA content in islets

Chronic (24 h) exposure to rapamycin (10, 30, and 100 nM) concentration dependently suppressed 16·7 mM glucose-induced insulin release (1·94±0·09, 10 nM; 1·65±0·06, 30 nM; 1·50±0·06, 100 nM rapamycin versus 2·35 ±0·11 ng/islet per 30 min, control, $n=30$, $P<0·01$ respectively) but did not affect basal insulin release in the presence of 2·8 mM glucose (Fig. 1A). Insulin secretion divided by insulin content also demonstrates that rapamycin suppresses glucose-induced insulin secretion (Fig. 1A). Insulin and DNA contents were not affected by 24-h exposure to 10, 30, and 100 nM rapamycin (Table 1), indicating that these concentrations of rapamycin do not reduce islet β-cell mass. Reactive oxygen species (ROS) scavengers did not affect suppressed glucose-induced insulin secretion by rapamycin (1·60±0·10, 30 nM rapamycin versus 1·69±0·10 ng/islet per 30 min, 30 nM rapamycin with α-tocopherol plus ascorbate, $n=10$, not significant).

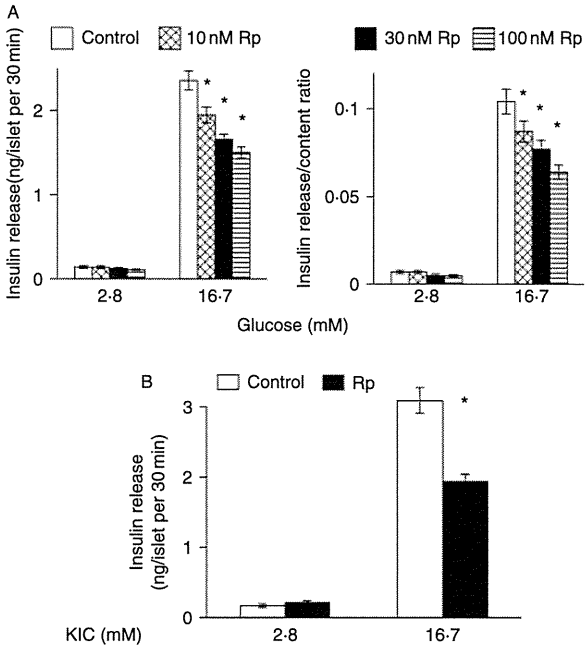

Figure 1 Effects of chronic exposure to rapamycin (Rp) on fuel secretagogue-induced insulin release from islets. (A) High (16·7 mM) glucose-induced and basal insulin release in control and Rp-treated islets. Islets were cultured with 10, 30, and 100 nM Rp or without Rp for 24 h. After cultured islets were preincubated with 2·8 mM glucose for 30 min, they were incubated with 2·8 and 16·7 mM glucose. Insulin secretions are presented as insulin secretion for 30 min/islet (right) and as the ratio of insulin secretion for 30 min to insulin content (left). Values represent mean±S.E.M. of 30 determinations. *$P<0·01$ versus corresponding control. (B) High KIC (16·7 mM)-induced and basal insulin release in control and Rp-treated islets. Islets were cultured with or without 30 nM Rp for 24 h. After cultured islets were preincubated with 2·8 mM glucose for 30 min, they were incubated with 2·8 and 16·7 mM KIC. Values represent mean±S.E.M. of 18 determinations. *$P<0·01$ versus corresponding control.

Table 1 Effect of chronic exposure to rapamycin on insulin content and DNA content. At the end of experiments indicated in Fig. 1A, insulin content and DNA content in islets were determined. Values represent mean±S.E.M. of 60 determinations

	Insulin content (ng/islet)	DNA content (ng/islet)
Experimental condition during culture		
Control	24·7±1·0	14·6±0·4
10 nM rapamycin	24·1±1·0	14·5±0·4
30 nM rapamycin	24·5±1·1	15·0±0·5
100 nM rapamycin	23·7±0·8	14·1±0·3

Effect of chronic exposure to rapamycin on KIC-induced insulin release

To characterize metabolic fuel-induced insulin release independent of glycolysis, KIC-induced insulin release from rapamycin-treated islets was examined. Chronic exposure to 30 nM rapamycin decreased high KIC-induced insulin release (1·93±0·10, rapamycin versus 3·09±0·18 ng/islet per 30 min, control, $n=18$, $P<0·01$; Fig. 1B).

Effect of rapamycin on ATP content

ATP content was greater in control islets incubated with 16·7 mM glucose than in control islets incubated with 2·8 mM glucose (11·97±0·35, 2·8 mM glucose versus 16·04±0·46 pmol/islet, 16·7 mM glucose, $n=30$, $P<0·01$; Fig. 2). ATP content in the presence of 16·7 mM glucose

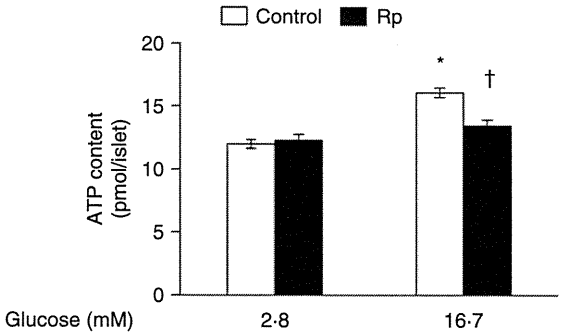

Figure 2 Effects of chronic exposure to rapamycin (Rp) on ATP contents in islets. Islets were cultured with or without 30 nM Rp for 24 h. After cultured islets were preincubated with 2·8 mM glucose for 30 min, and then incubated with 2·8 and 16·7 mM glucose for 30 min, ATP contents were determined. Values represent mean ±S.E.M. of 30 determinations. *$P<0·01$ versus control with 2·8 mM glucose. †$P<0·01$ versus control with 16·7 mM glucose.

was significantly reduced in rapamycin-treated islets (13·42 ±0·47 pmol/islet, 16·7 mM glucose, rapamycin versus 16·7 mM glucose, control, $n=30$, $P<0·01$), but that in the presence of 2·8 mM glucose was not affected by rapamycin (Fig. 2). ROS scavengers did not affect the suppressed ATP content in the presence of high glucose by rapamycin (13·27 ±0·92, 30 nM rapamycin versus 14·58±0·82 pmol/islet, 30 nM rapamycin with α-tocopherol plus ascorbate, $n=10$, not significant).

Effects of rapamycin on glucose utilization and glucose oxidation

Glucose utilization was greater in islets incubated with 16·7 mM glucose than that in islets incubated with 2·8 mM glucose in both control (33·0±1·8, 2·8 mM glucose versus 98·4±5·0 pmol/islet per 90 min, 16·7 mM glucose, $n=15$, $P<0·01$) and rapamycin-treated islets (28·1±1·7, 2·8 mM glucose versus 75·1±2·6 pmol/islet per 90 min, 16·7 mM glucose, $n=15$, $P<0·01$). Glucose utilization in the presence of 16·7 mM glucose was significantly reduced in rapamycin-treated islets ($P<0·01$), but that in the presence of 2·8 mM glucose was not affected by rapamycin (Fig. 3A).

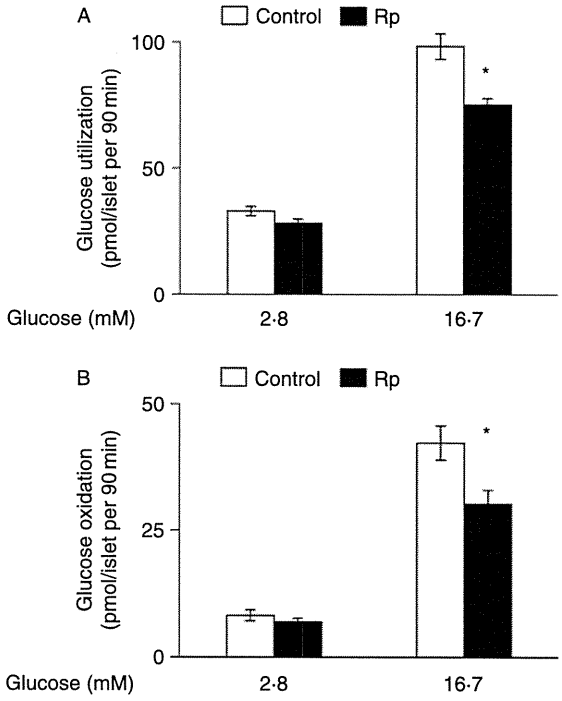

Figure 3 Effects of chronic exposure to rapamycin (Rp) on glucose utilization and oxidation in islets. Islets were cultured with or without 30 nM Rp for 24 h. After cultured islets were preincubated with 2·8 mM glucose for 30 min, they were incubated with 2·8 and 16·7 mM glucose for 90 min. (A) Glucose utilization. Values represent mean±S.E.M. of 15 determinations. *$P<0·01$ versus corresponding control. (B) Glucose oxidation. Values represent mean±S.E.M. of nine determinations. *$P<0·01$ versus corresponding control.

Glucose oxidation was greater in islets incubated with 16·7 mM glucose than that in islets incubated with 2·8 mM glucose in both control (8·1±1·1, 2·8 mM glucose versus 42·2±3·3 pmol/islet per 90 min, 16·7 mM glucose, $n=9$, $P<0·01$) and rapamycin-treated islets (6·8±0·7, 2·8 mM glucose versus 30·1±2·7 pmol/islet per 90 min, 16·7 mM glucose, $n=9$, $P<0·01$). Glucose oxidation in the presence of 16·7 mM glucose was significantly reduced in rapamycin-treated islets ($P<0·01$), but that in the presence of 2·8 mM glucose was not affected by rapamycin (Fig. 3B). Glucose oxidation in the presence of 16·7 mM glucose declined 77% by 100 nM antimycin A, which is comparable with the reduction by rapamycin treatment. In the same condition, glucose utilization with high glucose also declined 78% by antimycin A (Table 2).

Effect of rapamycin on glucokinase activity

Glucokinase activity was not affected by rapamycin treatment (87·4±10·4, rapamycin versus 75·4±14·8 pmol/islet per 60 min, control, $n=3$, not significant).

Effect of rapamycin on expression of mitochondrial respiratory chain complexes

Immunoblotting using lysates of whole islets revealed that rapamycin did not affect expression of complex I, III, IV, and V of the mitochondrial respiratory chain proteins (Fig. 4).

Effect of rapamycin on ATP production by mitochondria from islets

ATP production by mitochondria from control and rapamycin-cultured islets in the presence of various substrates and inhibitors is shown in Table 3. Antimycin A, a complex III inhibitor in the respiratory chain, inhibited ATP production dramatically in the presence of succinate in mitochondria from both control and rapamycin-cultured islets. Mitochondrial ATP production of rapamycin-cultured islets was similar to that of control islets in the presence of

Table 2 Effect of antimycin A on glucose oxidation and glucose utilization. Islets were cultured without rapamycin for 24 h. After cultured islets were preincubated with 2·8 mM glucose for 30 min, they were incubated with 2·8 and 16·7 mM glucose for 90 min with or without 100 nM antimycin A. Values represent mean±S.E.M. of nine (glucose oxidation) and five (glucose utilization) determinations

	Control	100 nM antimycin A
Glucose oxidation		
2·8 mM glucose	9·8±0·5	9·8±0·7
16·7 mM glucose	42·1±1·8	32·8±1·8*
Glucose utilization		
2·8 mM glucose	32·9±3·3	31·1±2·4
16·7 mM glucose	97·9±5·6	76·7±6·5†

*$P<0·01$ versus control without antimycin A. †$P<0·05$ versus control without antimycin A.

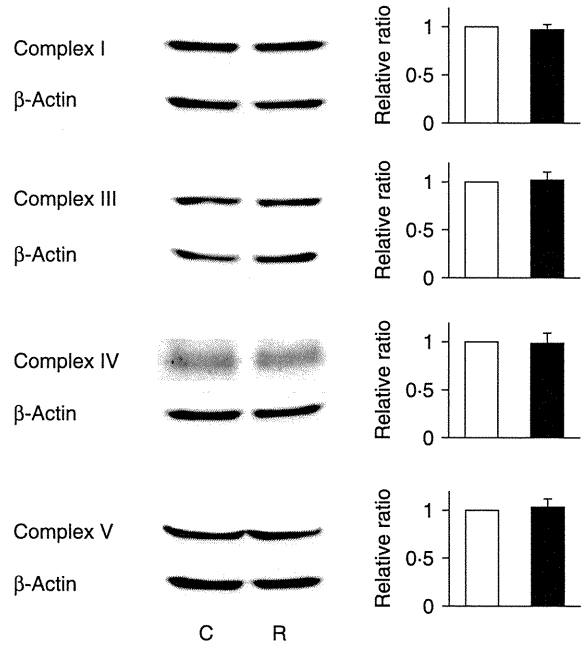

Figure 4 Immunoblots of complex I, III, VI, and V of mitochondrial respiratory chain proteins using lysates of whole-rat pancreatic islets. Islets were cultured with or without 30 nM rapamycin for 24 h. C, control; R, rapamycin. Quantification data from several independent experiments (I, $n=4$; III, $n=4$; VI, $n=3$; V, $n=4$) are also indicated. Open bar, control; closed bar, rapamycin. Data are expressed relative to control (without rapamycin) values corrected by β-actin level to eliminate influence of subtle difference in amount of loaded protein (means±S.E.M).

succinate plus rotenone, TMPD plus ascorbate, and glycerol-3-phosphate. ATP production by mitochondria from rapamycin-cultured islets in the presence of pyruvate plus malate was decreased compared with that from control islets.

α-Keto-β-methyl-*n*-valeric acid (KMV), a specific competitive inhibitor of KGDH, dose dependently suppressed mitochondrial ATP production in the presence of malate and pyruvate (Fig. 5).

Effect of rapamycin on activities of mitochondrial enzymes

Enzyme activities in the Krebs cycle including PDH, NAD-ICDH, aconitase, and MDH were not affected, but KGDH activity was reduced by rapamycin treatment (Table 4).

Discussion

In the present study, we show that rapamycin suppresses high glucose-induced insulin secretion from pancreatic islets by reducing mitochondrial ATP production through suppression of carbohydrate metabolism in the Krebs cycle, together with reduced KGDH activity. Thus, dysfunction in mitochondrial ATP production may be derived not from alteration in protein expression and dysfunction of the respiratory chain but from decreased KGDH activity that limits the velocity of carbohydrate metabolism in the Krebs cycle.

Rapamycin significantly decreased glucose-induced insulin release after 1 to several days exposure, as found in previous studies using rat islets (Bell *et al.* 2003) and mice islets (Zhang *et al.* 2006). In the present study, exposure to 30 nM rapamycin for 24 h reduced glucose-induced insulin release without affecting insulin and DNA content, which indicates that reduced insulin release by rapamycin is not necessarily derived from reduced β-cell mass, while rapamycin above 10 nM was found to increase apoptosis in MIN-6 cells in a previous study (Bell *et al.* 2003). To investigate the mechanism of reduced insulin release by rapamycin independent of reduced insulin and DNA content, we used 30 nM rapamycin-treated islets. The recommended trough concentrations of rapamycin in blood are 5–15 ng/ml (or 5·5–15·9 nM) in islet transplantation (Shapiro *et al.* 2000) and renal transplantation (Teutonico *et al.* 2005). Accordingly, the concentration used in our experiments was two to six times clinically used trough concentrations.

In pancreatic β-cells, intracellular ATP originated mainly from mitochondria is one of the most important regulators of insulin secretion (Maechler & Wollheim 2001). Glucose entry into the β-cells accelerates glycolysis and mitochondrial carbohydrate metabolism that increases ATP content and ATP/ADP ratio, which closes the ATP-sensitive K^+ channels (K_{ATP} channel). The decrease in K^+ conductance depolarizes the membrane and opens the voltage-dependent Ca^{2+} channels (VDCCs). Increased Ca^{2+} influx through VDCCs increases the intracellular Ca^{2+} concentration to a level that triggers

Table 3 ATP production by mitochondria from control and rapamycin (Rp)-cultured islets. Islets were cultured with or without 30 nM Rp for 24 h. Mitochondrial suspension was obtained from control and Rp-cultured islets. Mitochondrial ATP production is indicated as the ratio to ATP production from adenylate kinase, which was determined from the same sample in parallel incubation. Values represent mean±S.E.M. of five (A) and three (B) determinations

	Mitochondrial ATP production	
Experimental conditions	Control islets	Rp-cultured islets
A		
1 mM succinate+1 μM rotenone	6·40±0·32	6·47±0·44
1 mM pyruvate+1 mM malate	3·22±0·10	2·69±0·11*
0·5 mM TMPD+2 mM ascorbate	8·74±1·44	8·70±1·34
1 mM glycerol-3-phosphate	0·66±0·13	0·55±0·08
1 mM succinate+1 μM antimycin A	0·02±0·00	0·02±0·00
B		
1 mM succinate	7·13±0·12	ND
1 mM succinate+1 μM rotenone	6·39±0·06	ND
1 mM succinate+1 μM antimycin A	0·02±0·01	ND
1 mM succinate+1 μM rotenone+1 μM antimycin A	0·03±0·00	ND

*$P<0·05$ versus corresponding control cultured without Rp. TMPD, tetramethyl-*p*-phenyldiamine. ND, not determined.

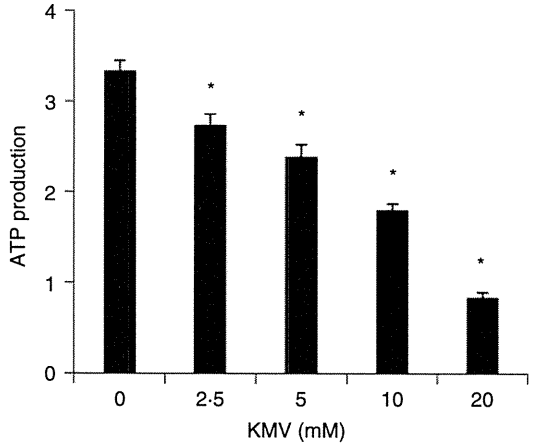

Figure 5 Effect of α-keto-β-methyl-*n*-valeric acid (KMV) on mitochondrial ATP production. Islets were cultured for 24 h. Mitochondrial suspension was obtained from cultured islets. Mitochondrial ATP production in the presence of 1 mM pyruvate and 1 mM malate with various concentrations of KMV is indicated as the ratio to ATP production from adenylate kinase, which was determined from the same sample in parallel incubation. Values represent mean±S.E.M. of six determinations. *$P<0·01$ versus control without KMV.

exocytosis of the insulin granules. Moreover, ATP directly affects the exocytotic system and enhances insulin release in experiments using single β-cells (Rorsman 1997, Takahashi *et al.* 1999) and permeabilized islets (Fujimoto *et al.* 2002). Thus, a lower ATP level in the presence of high glucose plays a major role in the attenuation of insulin secretion from rapamycin-treated islets in response to high glucose.

In pancreatic islets, KIC is oxidized, enhancing ATP production and triggering insulin release (Malaisse *et al.* 1981), and two distinct mechanisms of KIC-induced insulin release are proposed. In one, KIC, which is converted to acetyl CoA via a branched chain α-keto acid dehydrogenase (BCKDH) -dependent pathway, enters into the Krebs cycle and is oxidized (Lenzen *et al.* 1982, 1985). In the other, KIC together with endogenous glutamate is converted to α-ketoglutarate via glutamate-keto acid transaminase (GKAT), which enters into the Krebs cycle and is oxidized (Gao *et al.* 2003). Because both BCKDH and GKAT are mitochondrial enzymes, KIC might well be metabolized within mitochondria without affecting cytosolic glycolysis, which is compatible with the results showing that inhibition of glycolysis by glucokinase inhibitor and glyceraldehyde-3-phosphate dehydrogenase inhibitor decreased glucose-induced insulin release, but did not affect KIC-induced insulin release (Radu *et al.* 2005). Reduced KIC-induced insulin release by rapamycin suggests that the decreased glucose metabolism may be derived from reduced mitochondrial carbohydrate metabolism.

Table 4 Effect of rapamycin (Rp) on enzyme activities in the Krebs cycle. Islets were cultured with or without 30 nM Rp for 24 h. Enzyme activities were measured using homogenates of mitochondrial fraction obtained from control and Rp-cultured islets. Values represent mean±S.E.M. of five determinations

	Enzyme activities (nmol/mg mitochondrial protein per min)	
	Control islets	Rp-cultured islets
PDH	10·64±0·38	10·98±0·38
Aconitase	10·83±0·78	9·77±0·78
NAD-ICDH	11·50±0·28	10·99±0·30
KGDH	13·82±0·84	10·08±0·82*
MDH	1116±37	1127±37

*$P<0·05$ versus corresponding control cultured without Rp. PDH, pyruvate dehydrogenase; NAD-ICDH, NAD^+ linked-isocitrate dehydrogenase; KGDH, α-ketoglutarate dehydrogenase; MDH, malate dehydrogenase.

Because rapamycin reduced glucose utilization in the presence of high glucose, which reflects the velocity of glycolysis (Meglasson & Matschinsky 1986), the activity of glucokinase, a rate-limiting enzyme in glycolysis (Matschinsky 1996), was examined. Since rapamycin treatment did not affect glucokinase activity in islets, the primary cause of reduced glucose oxidation by the treatment is not likely to be reduced the velocity of glycolysis. Indeed, in islets, glucose utilization is also reduced when glucose oxidation is decreased by respiratory chain inhibitors including site III inhibitor in our results and site VI inhibitor (Sener *et al.* 2007), suggesting that reduced glucose oxidation may decrease glucose utilization. Since glucokinase is a unique hexokinase, which lacks product inhibition (Matschinsky 2002), accumulation of glucose-6-phosphate by mitochondrial metabolic inhibition may not participate in glycolysis inhibition. Moreover, since K_m of glucokinase for ATP is about 0·5 mM, which is less than the estimated cytosolic ATP concentration with a basal level of glucose in β-cells (about 3 mM; Meglasson & Matschinsky 1984), a decrease in the cytosolic ATP concentration by mitochondrial metabolic inhibition may have little effect on velocity of glycolysis.

Mitochondrial ATP production is driven by the H^+ gradient across the mitochondrial membrane generated by transport of high-energy electrons in the respiratory chain. These electrons are derived from NADH and $FADH_2$ derived from the Krebs cycle in the matrix and/or transferred from the cytosol by the shuttle system. To find the defective site in mitochondrial carbohydrate metabolism in rapamycin-cultured islets, mitochondrial ATP production was examined in the presence of various substrates and inhibitors. As ATP production in the presence of glycerol phosphate was not affected, reduced function of the glycerol phosphate shuttle, which is observed in diabetic islets (Östenson *et al.* 1993), may not participate in the reduction of ATP production by rapamycin treatment. In the presence of rotenone, a complex I inhibitor, and succinate, which renders electrons indirectly to complex I via the Krebs cycle and directly to complex II, electrons are rendered to the respiratory chain via $FADH_2$ at complex II and not at complex I via NADH, which is derived from metabolism in the Krebs cycle. TMPD is an artificial

electron donor that can transfer electrons to cytochrome *c*. TMPD reduced by ascorbate renders electrons to cytochrome *c*, which transfers electrons to complex IV. The fact that ATP production in the presence of succinate plus rotenone and in the presence of TMPD plus ascorbate is similar in the two groups of mitochondria indicates that the respiratory chain downstream of complex II is not affected by chronic exposure to rapamycin. Moreover, immunoblotting revealed that expressions of respiratory chain proteins including complex I, III, IV, and V were not affected by rapamycin treatment. Antibodies used in the present study were raised against 39 kDa subunit in complex I, core II in complex III, subunit I in complex IV, and subunit α in complex V. In these subunits, subunit I in complex IV is derived from an mtDNA-encoded gene; the others are from nuclear genes (Hunte 2001, Richter & Ludwig 2003, Scheffler 2008, Zickermann *et al.* 2009), indicating that rapamycin does not affect the expression of respiratory proteins derived from mtDNA or nuclear genes in islets. Considered together, these results do not support the notion that rapamycin reduces ATP production by reducing activity of the respiratory chain. Because the decrease in ATP production was found in the presence of substrates that are metabolizable in the Krebs cycle by rapamycin treatment, the reduction in ATP production may be attributable to reduced carbohydrate metabolism in the Krebs cycle.

Glucose oxidation reflects the velocity of carbohydrate metabolism in the Krebs cycle in which CO_2 is released in the reaction mediated by dehydrogenases. To clarify the link between reduced mitochondrial ATP production in the presence of substrates metabolizable in the Krebs cycle and reduced glucose oxidation by rapamycin, recovery of insulin release and ATP content in the presence of high glucose by ROS scavengers and activity of enzymes in the Krebs cycle were examined. Ouabain-induced endogenous ROS suppresses mitochondrial metabolism in the Krebs cycle, subsequently reducing ATP production, and reduces glucose-induced insulin release and ATP levels in the presence of high glucose, which is recovered by the suppression of endogenous ROS production and by ROS scavenge (Kajikawa *et al.* 2002, Kominato *et al.* 2008). High glucose raises ROS level in β-cells (Bindokas *et al.* 2003, Sakai *et al.* 2003), which is also found in our previous study (Kominato *et al.* 2008). However, our previous study shows that ROS scavenging does not affect glucose-induced insulin secretion from control islets, but increases that from GK-diabetic islets. A more profound increase in high glucose-induced ROS was observed in diabetic islets compared with control islets. These results suggest that a physiological level of ROS increase by glucose does not impair stimulus-secretion coupling, while a pathophysiological increase in ROS impairs stimulus-secretion coupling. Administration of H_2O_2, the most abundant ROS, to mitochondria reduced the activity of Krebs cycle enzymes including aconitase, KGDH, and succinate dehydrogenase (Tretter & Adam-Vizi 2000, Nulton-Persson & Szweda 2001). Because α-tocopherol is a lipid-soluble antioxidant, it is often used as membrane-permeable ROS scavenger. α-tocopherol reduces ROS production in various kinds of cells (Saito *et al.* 2003, Brookheart *et al.* 2009, Yang *et al.* 2009) including β-cells (Kajikawa *et al.* 2002). As ascorbate is water soluble, it is not necessarily membrane permeable. However, it is useful to prevent oxidization of α-tocopherol in the medium and to maintain the ROS-scavenging effect of α-tocopherol. Because insulin release and ATP content in the presence of high glucose in rapamycin-treated islets were not increased by the addition of α-tocopherol plus ascorbate, overproduction of endogenous ROS seems not to participate in reduced mitochondrial carbohydrate metabolism due to rapamycin treatment.

Impaired metabolism-secretion coupling in β-cells due to reduced activity of enzymes in the Krebs cycle has been reported. Exposure to fatty acids for 48 h inhibits glucose-induced insulin secretion from islets with decreased activity in PDH (Zhou & Grill 1995). Interleukin-1β-induced nitric oxide production leads to inhibition of glucose-induced insulin secretion together with reduced aconitase activity (Welsh *et al.* 1991). In the present study, activity of KGDH was decreased by rapamycin treatment. The reaction catalyzed by KGDH is one of the slowest steps in the Krebs cycle, and thus can be the rate-limiting step in islets (Ashcroft 1981) and in other tissues (Tretter & Adam-Vizi 2000, Nulton-Persson & Szweda 2001). Inhibition of KGDH alters mitochondrial function in N2a neuroblastoma cells (Huang *et al.* 2003). These findings suggest that decreased activity of KGDH might reduce mitochondrial ATP production and result in decreased glucose-induced insulin secretion from rapamycin-treated islets. To investigate this, suppression of mitochondrial ATP production by inhibition of KGDH was examined using KMV, a specific competitive inhibitor of KGDH (Huang *et al.* 2003). KMV dose dependently suppressed mitochondrial ATP production in the presence of malate and pyruvate. This dose dependency of KMV on mitochondrial ATP production is consistent with the dose-dependent effect of KMV on KGDH activities previously described (Huang *et al.* 2003). These results indicate that reaction at KGDH may limit the velocity of carbohydrate metabolism in the Krebs cycle and thus mitochondrial ATP production, which is consistent with the result that KGDH limits the amount of NADH available for the respiratory chain (Tretter & Adam-Vizi 2000). These results support the notion that a slight alteration in KGDH activity may affect mitochondrial ATP production.

While rapamycin shares with tacrolimus a similar molecular structure and binding ability to FK-binding protein 12 (FKBP12), the FKBP12–rapamycin complex has no effect on calcineurin, a phosphatase that is known to be inhibited by the FKBP12–tacrolimus complex (Saunders *et al.* 2001). This is consistent with our finding in the present study that rapamycin had no effect on glucokinase activity, but tacrolimus suppresses glucokinase activity in islets (Radu *et al.* 2005). MTOR has an FKBP12–rapamycin binding domain to which phosphatidic acid (PA) can also bind.

MTOR expresses biological effects by forming two types of complexes, MTORC1 and MTORC2, which includes MTOR and PA commonly and Raptor and Rictor respectively. FKBP12–rapamycin is believed to inhibit MTOR signaling by preventing the interaction between MTOR and PA and thus forming MTOR complexes (Foster & Toschi 2009). Since low concentrations of rapamycin (0·5–100 nM) target MTORC1 and higher concentrations of rapamycin (0·2–20 μM) target MTORC2 (Foster & Toschi 2009), our result may be derived from inhibition of signaling mediated by MTORC1.

Recently, it has been revealed that MTOR is a nutrient sensor that balances energy metabolism by transcriptional control of mitochondrial oxidative function using peroxisome proliferator-activated receptor γ coactivator-1α in skeletal muscle cells (Cunningham *et al.* 2007). Further investigation of suppression of KGDH activity by rapamycin is required to clarify adaptation of mitochondrial oxidative function and insulin secretion according to nutrient supply.

Declaration of interest

The authors declare that there is no conflict of interest that would prejudice the impartiality of this scientific work.

Funding

This study was supported by Scientific Research Grants, a Grant for Leading Project for Biosimulation from the Ministry of Education, Culture, Sports, Science, and Technology of Japan, and a grant from CREST of Japan Science and Technology Cooperation.

Acknowledgements

The authors thank Mr T Yamaguchi and Ms C Kotake for their technical assistance.

References

Ashcroft SJH 1981 Metabolic control of insulin secretion. In *The Islets of Langerhans: Biochemistry, Physiology, and Pathology*, pp 117–148. Eds SJ Cooperstein & D Watkins. New York: Academic Press.

Bell E, Cao X, Moibi JA, Greene SR, Young R, Trucco M, Gao Z, Matschinsky FM, Deng S, Markman JF *et al.* 2003 Rapamycin has a deleterious effect on MIN-6 cells and rat and human islets. *Diabetes* **52** 2731–2739.

Bindokas VP, Kuznetsov A, Sreenan S, Polonsky KS, Roe MW & Philipson LH 2003 Visualizing superoxide production in normal and diabetic rat islets of Langerhans. *Journal of Biological Chemistry* **278** 9796–9801.

Brookheart RT, Michel CI, Listenberger LL, Ory DS & Schaffer JE 2009 The non-coding RNA gadd7 is a regulator of lipid-induced oxidative and endoplasmic reticulum stress. *Journal of Biological Chemistry* **284** 7446–7454.

Cho HJ, Park J, Lee HW, Lee YS & Kim JB 2004 Regulation of adipocyte differentiation and insulin action with rapamycin. *Biochemical and Biophysical Research Communications* **321** 942–948.

Cunningham JT, Rodgers JT, Arlow DH, Vazquez F, Mootha VK & Puigserver P 2007 mTOR controls mitochondrial oxidative function through a YY1-PGC-1α transcriptional complex. *Nature* **450** 736–740.

Foster DA & Toschi A 2009 Targeting mTOR with rapamycin: one dose does not fit all. *Cell Cycle* **8** 1026–1029.

Fraenkel M, Ketzinel-Gilad M, Ariav Y, Pappo O, Karaca M, Castel J, Berthault MF, Magnan C, Cerasi E, Kaiser N *et al.* 2008 mTOR inhibition by rapamycin prevents β-cell adaptation to hyperglycemia and exacerbates the metabolic state in type 2 diabetes. *Diabetes* **57** 945–957.

Fujimoto S, Ishida H, Kato S, Okamoto Y, Tsuji K, Mizuno N, Ueda S, Mukai E & Seino Y 1998 The novel insulinotropic mechanism of pimobendan: direct enhancement of the exocytotic process of insulin secretory granules by increased Ca^{2+} sensitivity in β-cells. *Endocrinology* **139** 1133–1140.

Fujimoto S, Tsuura Y, Ishida H, Tsuji K, Mukai E, Kajikawa M, Hamamoto Y, Takeda T, Yamada Y & Seino Y 2000 Augmentation of basal insulin release from rat islets by preexposure to a high concentration of glucose. *American Journal of Physiology* **279** E927–E940.

Fujimoto S, Mukai E, Hamamoto Y, Takeda T, Takehiro M, Yamada Y & Seino Y 2002 Prior exposure to high glucose augments depolarization-induced insulin release by mitigating the decline of ATP level in rat islets. *Endocrinology* **143** 213–221.

Fujimoto S, Nabe K, Takehiro M, Shimodahira M, Kajikawa M, Takeda T, Mukai E, Inagaki N & Seino Y 2007 Impaired metabolism-secretion coupling in pancreatic β-cells: role of determinants of mitochondrial ATP production. *Diabetes Research and Clinical Practice* **77** S2–S10.

Gao Z, Young RA, Li G, Najafi H, Buettger C, Sukumvanich SS, Wong RK, Wolf BA & Matschinsky FM 2003 Distinguishing features of leucine and α-ketoisocaproate sensing in pancreatic β-cells. *Endocrinology* **144** 1949–1957.

Huang HM, Zhang H, Xu H & Gibson GE 2003 Inhibition of the α-ketoglutarate dehydrogenase complex alters mitochondrial function and cellular calcium regulation. *Biochimica et Biophysica Acta* **1637** 119–126.

Hunte C 2001 Insights from the structure of the yeast cytochrome bc1 complex: crystallization of membrane proteins with antibody fragments. *FEBS Letters* **504** 126–132.

Kajikawa M, Fujimoto S, Tsuura Y, Mukai E, Takeda T, Hamamoto Y, Takehiro M, Fujita J, Yamada Y & Seino Y 2002 Ouabain suppresses glucose-induced mitochondrial ATP production and insulin release by generating reactive oxygen species in pancreatic islets. *Diabetes* **51** 2522–2529.

Kennedy ED, Maechler P & Wollheim CB 1998 Effects of depletion of mitochondrial DNA in metabolism secretion coupling in INS-1 cells. *Diabetes* **47** 374–380.

Kominato R, Fujimoto S, Mukai E, Nakamura Y, Nabe K, Shimodahira M, Nishi Y, Funakoshi S, Seino Y & Inagaki N 2008 Src activation generates reactive oxygen species and impairs metabolism-secretion coupling in diabetic Goto-Kakizaki and ouabain-treated rat pancreatic islets. *Diabetologia* **51** 1226–1235.

Lenzen S, Formanek H & Panten U 1982 Signal function of metabolism of neutral amino acids and 2-keto acids for initiation of insulin secretion. *Journal of Biological Chemistry* **257** 6631–6633.

Lenzen S, Schmidt W & Panten U 1985 Transamination of neutral amino acids and 2-keto acids in pancreatic B-cell mitochondria. *Journal of Biological Chemistry* **260** 12629–12634.

Lu X, Schuurman HJ & Borel JF 1994 Effect of rapamycin on islet xenograft survival. *Transplantation Proceedings* **26** 1128–1129.

Maechler P & Wollheim CB 2001 Mitochondrial function in normal and diabetic β-cells. *Nature* **414** 807–812.

Malaisse WJ, Sener A, Malaisse-Legae F, Hutton JC & Christophe J 1981 The stimulus-secretion coupling of amino acid-induced insulin release. Metabolic interaction of L-glutamine and 2-ketoisocaproate in pancreatic islets. *Biochimica et Biophysica Acta* **677** 39–49.

Matschinsky FM 1996 Banting Lecture 1995. A lesson in metabolic regulation inspired by the glucokinase glucose sensor paradigm. *Diabetes* **45** 223–241.

Matschinsky FM 2002 Regulation of pancreatic β-cell glucokinase. *Diabetes* **51** S394–S404.

McDaniel ML, Marshall CA, Pappan KL & Kwon G 2002 Metabolic and autocrine regulation of the mammalian target of rapamycin by pancreatic β-cells. *Diabetes* **51** 2877–2885.

Meglasson MD & Matschinsky FM 1984 New perspectives on pancreatic islet glucokinase. *American Journal of Physiology* **246** E1–E13.

Meglasson MD & Matschinsky FM 1986 Pancreatic islet glucose metabolism and regulation of insulin secretion. *Diabetes/Metabolism Reviews* **2** 163–214.

Nabe K, Fujimoto S, Shimodahira M, Kominato R, Nishi Y, Funakoshi S, Mukai E, Yamada Y, Seino Y & Inagaki N 2006 Diphenylhydantoin suppresses glucose-induced insulin release by decreasing cytoplasmic H^+ concentration in pancreatic islets. *Endocrinology* **147** 2717–2727.

Nulton-Persson AC & Szweda LI 2001 Modulation of mitochondrial function by hydrogen peroxide. *Journal of Biological Chemistry* **276** 23357–23361.

Östenson CG, Abdel-Halim SM, Rasschaert J, Malaisse-Lagae F, Meuris S, Sener A, Efendic S & Malaisse WJ 1993 Deficient activity of FAD-linked glycerophosphate dehydrogenase in islets of GK rats. *Diabetologia* **36** 722–726.

Radu RG, Fujimoto S, Mukai E, Takehiro M, Shimono D, Nabe K, Shimodahira M, Kominato R, Aramaki Y, Nishi Y *et al.* 2005 Tacrolimus suppresses glucose-induced insulin release from pancreatic islets by reducing glucokinase activity. *American Journal of Physiology* **288** E372–E380.

Richter OM & Ludwig B 2003 Cytochrome *c* oxidase – structure, function, and physiology of a redox-driven molecular machine. *Reviews of Physiology, Biochemistry and Pharmacology* **147** 47–74.

Rorsman P 1997 The pancreatic β-cell as a fuel sensor: an electrophysiologist's viewpoint. *Diabetologia* **40** 487–495.

Saito Y, Yoshida Y, Akazawa T, Takahashi K & Niki E 2003 Cell death caused by selenium deficiency and protective effect of antioxidants. *Journal of Biological Chemistry* **278** 39428–39434.

Sakai K, Matsumoto K, Nishikawa T, Suefuji M, Nakamaru K, Hirashima Y, Kawashima J, Shirotani T, Ichinose K, Brownlee M *et al.* 2003 Mitochondrial reactive oxygen species reduce insulin secretion by pancreatic β-cells. *Biochemical and Biophysical Research Communications* **300** 216–222.

Saunders RN, Metcalfe MS & Nicholson ML 2001 Rapamycin in transplantation: a review of the evidence. *Kidney International* **59** 3–16.

Scheffler IE 2008 Biogenesis of mitochondria and mitochondrial electron transfer and oxidative phosphorylation. In *Mitochondria*, edn 2, pp 60–297. Ed. IE Scheffler. Hoboken: John Wiley & Sons, Inc.

Schieke SM, Phillips D, McCoy JP Jr, Aponte AM, Shen RF, Balaban RS & Finkel T 2006 The mammalian target of rapamycin (mTOR) pathway regulates mitochondrial oxygen consumption and oxidative capacity. *Journal of Biological Chemistry* **281** 27643–27652.

Schwab MA, Kölker S, van den Heuvel LP, Sauer S, Wolf NI, Rating D, Hoffmann GF, Smeitink JA & Okun JG 2005 Optimized spectrophotometric assay for the completely activated pyruvate dehydrogenase complex in fibroblasts. *Clinical Chemistry* **51** 151–160.

Sener A, Jijakli H, Zahedi Asl S, Courtois P, Yates AP, Meuris S, Best LC & Malaisse WJ 2007 Possible role of carbonic anhydrase in rat pancreatic islets: enzymatic, secretory, metabolic, ionic, and electrical aspects. *American Journal of Physiology* **292** E1624–E1630.

Shapiro AM, Lakey JR, Ryan EA, Korbutt GS, Toth E, Warnock GL, Kneteman NM & Rajotte RV 2000 Islet transplantation in seven patients with type 1 diabetes mellitus using a glucocorticoid-free immunosuppressive regimen. *New England Journal of Medicine* **343** 230–238.

Simon N, Morin C, Urien S, Tillement JP & Bruguerolle B 2003 Tacrolimus and sirolimus decrease oxidative phosphorylation of isolated rat kidney mitochondria. *British Journal of Pharmacology* **138** 369–376.

Sipula IJ, Brown NF & Perdomo G 2006 Rapamycin-mediated inhibition of mammalian target of rapamycin in skeletal muscle cells reduces glucose utilization and increases fatty acid oxidation. *Metabolism* **55** 1637–1644.

Taha C, Liu Z, Jin J, Al-Hasani H, Sonenberg N & Klip A 1999 Opposite translational control of GLUT1 and GLUT4 glucose transporter mRNAs in response to insulin. Role of mammalian target of rapamycin, protein kinase B, and phosphatidylinositol 3-kinase in GLUT1 mRNA translation. *Journal of Biological Chemistry* **274** 33085–33091.

Takahashi N, Kadowaki T, Yazaki Y, Ellis-Davies GC, Miyashita Y & Kasai H 1999 Post-priming actions of ATP on Ca^{2+}-dependent exocytosis in pancreatic β cells. *PNAS* **96** 760–765.

Takehiro M, Fujimoto S, Shimodahira M, Shimono D, Mukai E, Nabe K, Radu RG, Kominato R, Aramaki Y, Seino Y *et al.* 2005 Chronic exposure to β-hydroxybutyrate inhibits glucose-induced insulin release from pancreatic islets by decreasing NADH contents. *American Journal of Physiology* **288** E365–E371.

Teutonico A, Schena PF & Di Paolo S 2005 Glucose metabolism in renal transplant recipients: effect of calcineurin inhibitor withdrawal and conversion to sirolimus. *Journal of the American Society of Nephrology* **16** 3128–3135.

Tretter L & Adam-Vizi V 2000 Inhibition of Krebs cycle enzymes by hydrogen peroxide: a key role of α-ketoglutarate dehydrogenase in limiting NADH production under oxidative stress. *Journal of Neuroscience* **20** 8972–8979.

Tsuruzoe K, Araki E, Furukawa N, Shirotani T, Matsumoto K, Kaneko K, Motoshima H, Yoshizato K, Shirakami A, Kishikawa H *et al.* 1998 Creation and characterization of a mitochondrial DNA-depleted pancreatic β-cell line: impaired insulin secretion induced by glucose, leucine, and sulfonylureas. *Diabetes* **47** 621–631.

Welsh N, Eizirik DL, Bendtzen K & Sandler S 1991 Interleukin-1 β-induced nitric oxide production in isolated rat pancreatic islets requires gene transcription and may lead to inhibition of the Krebs cycle enzyme aconitase. *Endocrinology* **129** 3167–3173.

Yang ZC, Wang KS, Wu Y, Zou XQ, Xiang YY, Chen XP & Li YJ 2009 Asymmetric dimethylarginine impairs glucose utilization via ROS/TLR4 pathway in adipocytes: an effect prevented by vitamin E. *Cellular Physiology and Biochemistry* **24** 115–124.

Zhang N, Su D, Qu S, Tse T, Bottino R, Balamurugan AN, Xu J, Bromberg JS & Dong HH 2006 Sirolimus is associated with reduced islet engraftment and impaired β-cell function. *Diabetes* **55** 2429–2436.

Zhou YP & Grill V 1995 Long term exposure to fatty acids and ketones inhibits B-cell functions in human pancreatic islets of Langerhans. *Journal of Clinical Endocrinology and Metabolism* **80** 1584–1590.

Zickermann V, Kerscher S, Zwicker K, Tocilescu MA, Radermacher M & Brandt U 2009 Architecture of complex I and its implications for electron transfer and proton pumping. *Biochimica et Biophysica Acta* **1787** 574–583.

Received in final form 16 September 2009
Accepted 7 October 2009
Made available online as an Accepted Preprint
7 October 2009

SHORT REPORT

Little enhancement of meal-induced glucagon-like peptide 1 secretion in Japanese: Comparison of type 2 diabetes patients and healthy controls

Daisuke Yabe[1]*, Akira Kuroe[1], Soushou Lee[2], Koin Watanabe[1], Takanori Hyo[1], Masahiro Hishizawa[1], Takeshi Kurose[1], Carolyn F Deacon[3], Jens J Holst[3], Tsutomu Hirano[2], Nobuya Inagaki[4], Yutaka Seino[1]

ABSTRACT

Although glucose-dependent insulinotropic polypeptide (GIP) levels have been characterized previously, GLP-1 levels in Asians remain unclear. Here, we investigate total and intact levels of GLP-1, as well as GIP during oral glucose and meal tolerance tests (OGTT and MTT) in Japanese patients with or without type 2 diabetes (T2DM). Seventeen Japanese healthy controls and 18 age-matched and untreated patients with T2DM of short duration participated in the present study. Fasting levels of total GPL-1 were similar between the two groups (approximately 15 pM), and intact GLP-1 levels were considerably low in both groups (less than 1 pM). In both groups, total GLP-1 reached a peak 30 min after glucose ingestion (30–40 pM), whereas intact GLP-1 levels remained low with no significant peak. In MTT, total and intact GLP-1 showed no obvious peak. The current data indicate that intact GLP-1 levels are considerably low in the Japanese and that meal-induced enhancement of GLP-1 secretion is negligible in the Japanese. (J Diabetes Invest, doi: 10.1111/j.2040-1124.2010.00010.x, 2010)

KEY WORDS: DPP-4, GIP, GLP-1

INTRODUCTION

Glucagon-like peptide-1 (GLP-1) and glucose-dependent insulinotropic peptide (GIP) are incretin hormones that are secreted from the gut in response to ingestion of nutrients and stimulate insulin secretion from pancreatic β cells[1–3]. On secretion, GLP-1 and GIP undergo rapid processing catalyzed by dipeptidyl peptidase-4 (DPP-4) and lose their ability to stimulate insulin secretion[1–3]. It is, therefore, of great importance to measure not only intact but also total (i.e. intact plus DPP-4-processed) forms of incretin hormones to study their secretion and processing *in vivo*, although assays for intact GLP-1 and GIP require specific antibodies and have not been widely available[4,5].

In healthy Caucasian subjects, incretin hormones contribute to more than half of the overall post-prandial insulin secretion[6–8], whereas a marked reduction in the incretin effect is characteristic of Caucasian patients with type 2 diabetes (T2DM)[8,9]. Although the precise mechanisms underlying the reduced incretin effect are not fully understood, approximately 20–30% reduction in post-prandial GLP-1 response[5,8], in addition to the diminished insulinotropic effect of GIP but not GLP-1[10], has been reported in Caucasian T2DM patients. Despite negligible GLP-1 deficiency in some studies[11–13], the present findings have led to the creation of GLP-1-based therapies, namely GLP-1 receptor agonists and DPP-4 inhibitors both of which correct the deficiency of endogenous intact GLP-1, thereby improving glycemic control in T2DM patients[14].

The GLP-1-based therapies have been more effective in Japanese T2DM patients than in other ethnicities[15–18], suggesting more profound GLP-1 deficiencies in Japanese T2DM patients. To address this possibility, we measured intact and total levels of GLP-1 as well as GIP in Japanese T2DM patients and healthy controls in response to glucose or meal ingestions.

MATERIALS AND METHODS

The protocol was approved by the ethics committee of each participating institute and written informed consent was obtained from all participants. A total of 35 subjects participated in the present study, of which 18 patients had T2DM (World Health Organization criteria) of relatively short duration (3.8 ± 0.7 years) and 17 controls did not have T2DM. None of the T2DM patients received any anti-diabetic drugs before the study. Characteristics of controls and T2DM are summarized in Table 1.

Participants were subjected to oral glucose and meal tolerance tests (OGTT and MTT) in the morning after an overnight fast on two separate days. For the tests, 75 g of glucose and a Japanese standard meal (480 kcal; carbohydrate:protein:fat = 2.8:1:1) were ingested within 5 and 10 min, respectively. As processing of intact GLP-1 and GIP by DPP-4 extinguishes their insulinotropic activities[2,3], the present study was designed to measure both intact and

[1]Division of Diabetes, Clinical Nutrition and Endocrinology, Kansai Electric Power Hospital, Osaka, [2]Department of Diabetes, Metabolism and Endocrinology, Showa University School of Medicine, Tokyo, Japan, [3]Department of Biomedical Sciences, University of Copenhagen, Copenhagen, Denmark, and [4]Department of Diabetes and Clinical Nutrition, Kyoto University Graduate School of Medicine, Kyoto, Japan
*Corresponding author. Dr Daisuke Yabe Tel.: +81-6-6458-5821 Fax: +81-6-6458-6994
E-mail address: ydaisuke-kyoto@umin.ac.jp
Received 23 October 2009; revised 14 December 2009; accepted 3 January 2010

Table 1 | Characteristics of healthy controls and patients with type 2 diabetes

	Control	T2DM
n	17	18
Female (%)	18	22
Age (years)	51 ± 3	55 ± 3
BMI (kg/m^2)	22.4 ± 0.6	23.9 ± 0.9
HbA1c (%)	5.2 ± 0.1	7.2 ± 0.5**
Duration (year)	–	3.8 ± 0.7
Systolic blood pressure (mmHg)	120 ± 3	124 ± 3
Diastolic blood pressure (mmHg)	77 ± 2	76 ± 2
Total cholesterol (mg/dL)	187 ± 8	205 ± 5
HDL cholesterol (mg/dL)	58 ± 5	58 ± 4
Triglycerides (mg/dL)	83 ± 8	137 ± 5*

Each value represents the mean ± SEM. BMI, body mass index; HDL, high-density lipoprotein; T2DM, patients with type 2 diabetes. *P < 0.01; **P < 0.05.

total (intact and DPP-4-processed) forms of GLP-1 and GIP. Catheters were placed in cubital veins and blood samples were withdrawn from the catheters directly into BD™ P700 Blood Collection Tubes (BD, Franklin Lakes, NJ, USA) containing a DPP-4 inhibitor to prevent DPP-4 processing. Aliquots of plasmas were extracted with ethanol at the final concentration of 70% (vol/vol) and dried extracts were reconstituted in the original volume prior to measuring incretin levels. Recoveries were 75–80% of the expected concentrations for intact and total GLP-1 added to plasmas before extraction, and 80–85% for intact and total GIP. Volumes of the reconstituted extracts used to measure incretins were as follows: total GLP-1 300 μL; intact GLP-1 40 μL; total GIP 150 μL; intact GIP 300 μL. All samples were measured in duplicate. Total GLP-1 was measured using antiserum 89390 specific for the amidated COOH-terminus of GLP-1, and detecting GLP-1(7–36)amide and GLP-1 (9–36)amide (detection limit: <1 pM)[19]. Intact GLP-1 was measured using a two-site sandwich enzyme-linked immunosorbent assay (ELISA) that detects GLP-1(7–36)amide and GLP-1(7–37), but not the NH2-terminally truncated metabolites, using two monoclonal antibodies, the near C-terminally directed GLP1F5 as a catching antibody and the strictly N-terminally directed Mab26.1 as a detecting antibody (detection limit, <0.5 pM)[5]. This assay has 100% cross-reactivity with GLP-1 (7–36)amide and 88% with GLP-1 (7–37), but <0.1% with either GLP-1 (9–36)amide or GLP-1 (9–37). Total GIP was measured using the COOH-terminally directed antiserum R65, reacting with intact GIP and GIP(3–42) but not with 8-kDa GIP, whose chemical nature and relationship to GIP secretion is uncertain (detection limit, 2 pM)[20]. Intact, biologically active GIP was measured using antiserum 98171, specific for the intact GIP and cross-reacting <0.1% with GIP(3–42) (detection limit, 5 pM)[4]. The intra- and inter-assay variations for intact GIP, total GIP and total GLP-1 radioimmunoassays were <6% and for intact GLP-1 ELISA was <5%. Levels of intact GLP-1 remained under the detection limit throughout the test in 4/15 T2DM/OGTT subjects, 6/17 control/OGTT subjects, 2/12 T2DM/MTT subjects and 3/16 control/MTT subjects. Subjects whose intact GLP-1 remained under the detection limit throughout the test were included in the current study and immeasurable values were regarded as zero. Proportions of such subjects were similar between the T2DM and the control group. Even when subjects whose intact GLP-1 remained under the detection limit throughout the test were excluded, levels of intact GLP-1 showed no significant difference between the T2DM and the control group.

Glucose levels were measured by standard procedures. Area under the curve (AUC) of each measurement was calculated according to the trapezoidal rule. All statistical calculations were carried out using StatView for Windows version 5.0 (SAS Institute, Berkeley, CA, USA). Two-way ANOVA for repeated measures with post-hoc analysis was used to analyze time-course curves. Values at single time-points were compared by unpaired *t*-test. A P value <0.05 was taken to indicate significant differences.

RESULTS

Fasting levels of total GLP-1 were 15.7 ± 1.0 and 15.5 ± 1.7 pM, and those of intact GLP-1 were 0.7 ± 0.2 and 0.2 ± 0.1 pM in the control and T2DM groups, respectively. In OGTT, total GLP-1 reached the peak (40.3 ± 10.4 and 35.3 ± 8.7 pM in the control and T2DM groups) 30 min after glucose was given, whereas intact GLP-1 levels remained low and showed no significant peak (Figure 1). AUC for total and intact GLP-1 were similar in the two groups. In MTT, total and intact GLP-1 showed no obvious peak. AUC for total and intact GLP-1 were also similar in the two groups. Fasting levels of total GIP were 21.2 ± 2.7 and 29.7 ± 8.0 pM, whereas those of intact GIP were 13.9 ± 2.8 and 13.8.0 ± 2.8 pM in the control and T2DM groups, respectively. In OGTT, total GIP reached the peak (141.7 ± 41.7 and 135.3 ± 36.3 pM in the control and T2DM groups) 30 min after glucose was given, and intact GIP reached the peak (51.2 ± 7.6 and 49.6 ± 8.2 pM in the control and T2DM groups) as early as 10 min after glucose was given. AUC for total and intact GIP in the two groups were similar. In MTT, total and intact GIP reached the peak (total: 183.6 ± 38.7 and 150.0 ± 18.4 pM and intact: 70.3 ± 10.2 and 72.9 ± 6.5 pM in the control and T2DM groups) 30 min after meal ingestion in both the control and T2DM groups. AUC for total and intact GIP were similar in the two groups.

DISCUSSION

In the present study, we determined total and intact levels of GLP-1 and GIP in healthy Japanese volunteers and untreated Japanese patients with T2DM of short duration in response to glucose or meal ingestion.

Intact GLP-1 levels were considerably low in not only the T2DM group but also the healthy volunteers. The very low levels of intact GLP-1 in the Japanese might be explained by impaired secretion from the gut, accelerated processing by DPP-4, or both. Intact GLP-1 levels remained very low despite the significant peak of total GLP-1 in response to glucose ingestion, suggesting enhanced GLP-1 processing by DPP-4. However, the intact

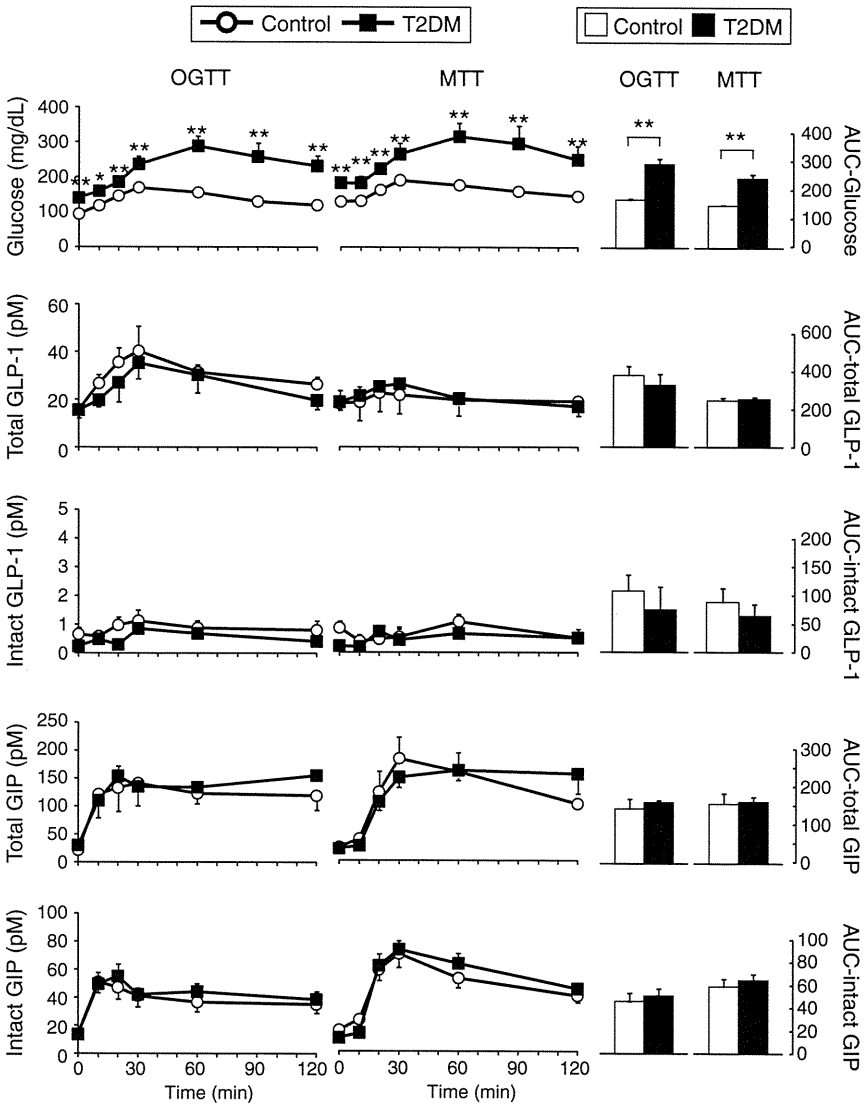

Figure 1 | Response of glucagon-like peptide 1 (GLP-1) and glucose-dependent insulinotropic polypeptide (GIP) after ingestion of oral glucose or a meal in Japanese patients with type 2 diabetes (T2DM) and healthy controls (Control). Japanese patients with T2DM and healthy controls were subjected to 75-g oral glucose and meal tolerance tests (OGTT and MTT). Left, levels of indicated measurements in each time-point (black squares, T2DM; white circles, control). Right, area under the curve (AUC) for indicated measurements were shown by arbitrary units (black bars, T2DM; white bars, control). Each value represents the mean ± SEM. *P < 0.05 and **P < 0.01 show that levels of T2DM are significantly different (unpaired t-test) from those of the control group at individual time-points. Numbers of subjects analyzed for glucose intact GLP-1 and intact GIP were as follows: T2DM/OGTT, n = 17; T2DM/MTT, n = 12; Control/OGTT, n = 15; Control/MTT, n = 16. Those analyzed for total GLP-1 and total GIP were as follows: T2DM/OGTT, n = 10; T2DM/MTT, n = 5; Control/OGTT, n = 9; Control/MTT, n = 10.

versus total ratio of GIP, another DPP-4 substrate, was much higher than that of GLP-1, implying that enhanced DPP-4 processing could be rather selective to GLP-1. Although GLP-1 has been shown to be more liable to DPP-4 processing than GIP[4], little is known about the kinetics of GLP-1 and GIP processing in the Japanese, and needs to be investigated in future to better understand the basis of the selective reduction of intact GLP-1.

Another important finding is that in the Japanese, the GLP-1 response after meal ingestion was negligible, despite the robust GIP response. The reduced GLP-1 response could be explained by meal size as well as meal composition, which was shown to be critical to GLP-1 response[21–23]. Regulatory mechanisms of nutrient-induced GLP-1 secretion are beginning to be shown[24] and further studies might shed light on the reduced meal-induced GLP-1 response in the Japanese.

Intact GLP-1 levels in the Japanese subjects in the current study were significantly lower than those of Caucasians reported

previously[5,25]. Although the same antibodies were used, intact GLP-1 levels in the Japanese and Caucasian subjects should not be compared because an ethanol extraction step was incorporated in the present study to reduce non-specific interference in plasma[26]. Characterizing a potential difference in the intact GLP-1 levels of Asians and Caucasians should be revisited by utilizing the exact same assay method.

Because there was no significant difference in the GLP-1 and GIP levels between the T2DM and control groups, incretin deficiency does not account for the reduced insulin response in Japanese T2DM patients in comparison with Japanese healthy volunteers. Nevertheless, the present study clearly showed that intact GLP-1 levels are considerably low in the Japanese and that GLP-1 response after ingestion of the Japanese standard meal is negligible in the Japanese, which might have implications for reduced insulin secretory capacity in the Japanese.

ACKNOWLEDGEMENT

No potential conflicts of interest relevant to this article were reported.

REFERENCES

1. Drucker DJ. The biology of incretin hormones. *Cell Metab* 2006; 3: 153–165.
2. Holst JJ. The physiology of glucagon-like peptide 1. *Physiol Rev* 2007; 87: 1409–1439.
3. Yamada Y, Miyawaki K, Tsukiyama K, *et al.* Pancreatic and extrapancreatic effects of gastric inhibitory polypeptide. *Diabetes* 2006; 55: S86–S91.
4. Deacon CF, Nauck MA, Meier J, *et al.* Degradation of endogenous and exogenous gastric inhibitory polypeptide in healthy and in type 2 diabetic subjects as revealed using a new assay for the intact peptide. *J Clin Endocrinol Metab* 2000; 85: 3575–3581.
5. Vilsboll T, Krarup T, Sonne J, *et al.* Incretin secretion in relation to meal size and body weight in healthy subjects and people with type 1 and type 2 diabetes mellitus. *J Clin Endocrinol Metab* 2003; 88: 2706–2713.
6. Nauck MA, Homberger E, Siegel EG, *et al.* Incretin effects of increasing glucose loads in man calculated from venous insulin and C-peptide responses. *J Clin Endocrinol Metab* 1986; 63: 492–498.
7. Shuster LT, Go VL, Rizza RA, *et al.* Incretin effect due to increased secretion and decreased clearance of insulin in normal humans. *Diabetes* 1988; 37: 200–203.
8. Muscelli E, Mari A, Casolaro A, *et al.* Separate impact of obesity and glucose tolerance on the incretin effect in normal subjects and type 2 diabetic patients. *Diabetes* 2008; 57: 1340–1348.
9. Nauck M, Stockmann F, Ebert R, *et al.* Reduced incretin effect in type 2 (non-insulin-dependent) diabetes. *Diabetologia* 1986; 29: 46–52.
10. Nauck MA, Heimesaat MM, Orskov C, *et al.* Preserved incretin activity of glucagon-like peptide 1 [7-36 amide] but not of synthetic human gastric inhibitory polypeptide in patients with type-2 diabetes mellitus. *J Clin Invest* 1993; 91: 301–307.
11. Orskov C, Jeppesen J, Madsbad S, *et al.* Proglucagon products in plasma of noninsulin-dependent diabetics and nondiabetic controls in the fasting state and after oral glucose and intravenous arginine. *J Clin Invest* 1991; 87: 415–423.
12. Ryskjaer J, Deacon CF, Carr RD, *et al.* Plasma dipeptidyl peptidase-IV activity in patients with type-2 diabetes mellitus correlates positively with HbAlc levels, but is not acutely affected by food intake. *Eur J Endocrinol* 2006; 155: 485–493.
13. Vollmer K, Holst JJ, Baller B, *et al.* Predictors of incretin concentrations in subjects with normal, impaired, and diabetic glucose tolerance. *Diabetes* 2008; 57: 678–687.
14. Lovshin JA, Drucker DJ. Incretin-based therapies for type 2 diabetes mellitus. *Nat Rev Endocrinol* 2009; 5: 262–269.
15. Amori RE, Lau J, Pittas AG. Efficacy and safety of incretin therapy in type 2 diabetes: systematic review and meta-analysis. *JAMA* 2007; 298: 194–206.
16. Kikuchi M, Abe N, Kato M, *et al.* Vildagliptin dose-dependently improves glycemic control in Japanese patients with type 2 diabetes mellitus. *Diabetes Res Clin Pract* 2009; 83: 233–240.
17. Nonaka K, Kakikawa T, Sato A, *et al.* Efficacy and safety of sitagliptin monotherapy in Japanese patients with type 2 diabetes. *Diabetes Res Clin Pract* 2008; 79: 291–298.
18. Seino Y, Rasmussen MF, Zdravkovic M, *et al.* Dose-dependent improvement in glycemia with once-daily liraglutide without hypoglycemia or weight gain: a double-blind, randomized, controlled trial in Japanese patients with type 2 diabetes. *Diabetes Res Clin Pract* 2008; 81: 161–168.
19. Orskov C, Rabenhoj L, Wettergren A, *et al.* Tissue and plasma concentrations of amidated and glycine-extended glucagon-like peptide I in humans. *Diabetes* 1994; 43: 535–539.
20. Krarup T, Holst JJ. The heterogeneity of gastric inhibitory polypeptide in porcine and human gastrointestinal mucosa evaluated with five different antisera. *Regul Pept* 1984; 9: 35–46.
21. Carr RD, Larsen MO, Winzell MS, *et al.* Incretin and islet hormonal responses to fat and protein ingestion in healthy men. *Am J Physiol Endocrinol Metab* 2008; 295: E779–E784.
22. Juntunen KS, Niskanen LK, Liukkonen KH, *et al.* Postprandial glucose, insulin, and incretin responses to grain products in healthy subjects. *Am J Clin Nutr* 2002; 75: 254–262.
23. Thomsen C, Rasmussen O, Lousen T, *et al.* Differential effects of saturated and monounsaturated fatty acids on postprandial lipemia and incretin responses in healthy subjects. *Am J Clin Nutr* 1999; 69: 1135–1143.
24. Tolhurst G, Reimann F, Gribble FM. Nutritional regulation of glucagon-like peptide-1 secretion. *J Physiol* 2009; 587: 27–32.
25. Meier JJ, Nauck MA, Kranz D, *et al.* Secretion, degradation, and elimination of glucagon-like peptide 1 and gastric inhibitory polypeptide in patients with chronic renal insufficiency and healthy control subjects. *Diabetes* 2004; 53: 654–662.
26. Deacon CF, Holst JJ. Immunoassays for the incretin hormones GIP and GLP-1. *Best Pract Res Clin Endocrinol Metab* 2009; 23: 425–432.

Original Paper

Neonatology
formerly Biology of the Neonate

Neonatology 2010;98:179–190
DOI: 10.1159/000283994

Received: June 30, 2009
Accepted after revision: December 10, 2009
Published online: March 16, 2010

Assessment of a New Piezoelectric Transducer Sensor for Noninvasive Cardiorespiratory Monitoring of Newborn Infants in the NICU

Shinichi Sato[a] Wako Ishida-Nakajima[b] Akira Ishida[b] Masanari Kawamura[b] Shinobu Miura[b] Kyoichi Ono[a] Nobuya Inagaki[c, d] Goro Takada[b] Tsutomu Takahashi[b]

Departments of [a]Cell Physiology and [b]Pediatrics, Akita University Graduate School of Medicine, Akita, [c]Department of Diabetes and Clinical Nutrition, Kyoto University Graduate School of Medicine, Kyoto, and [d]CREST of Japan Science and Technology Agency, Kawaguchi, Japan

Key Words

Cardiorespiratory monitoring, noninvasive · Piezoelectric transducer sensor · Heart sounds · Breathing movement · Motion artifact · Electrocardiogram · Impedance pneumography · Skin damage

Abstract

Background: Electrocardiogram (ECG) and impedance pneumography (IPG), the most widely used techniques for cardiorespiratory monitoring in the neonatal intensive care unit (NICU), have the disadvantage of causing skin damage when used for very premature newborn infants. To prevent skin damage, we designed a new piezoelectric transducer (PZT) sensor. ***Objective:*** To assess the potential of the PZT sensor for cardiorespiratory monitoring in the NICU. ***Methods:*** The PZT sensor was placed under a folded towel under a neonate to detect an acoustic cardiorespiratory signal, from which heart rate (HR) and breathing rate (BR) were calculated, together with simultaneous ECG/IPG recording for 1–9 days for long and brief (1-min) assessment. ***Results:*** The brief assessment showed average correlation coefficients of 0.92 ± 0.12 and 0.95 ± 0.02 between instantaneous HRs/BRs detected by the PZT sensor and ECG/IPG in 27 and 11 neonates examined. During the long assessment, the HR detection rate by the PZT sensor was ~10% lower than that by ECG (82.6 ± 12.9 vs. 91.8 ± 4.1%; p = 0.001, n = 27), although comparable (90.3 ± 4.1 vs. 92.5 ± 3.4%, p = 0.081) in ~70% (18/27) of neonates examined; BR detection rate was comparable between the PZT sensor and IPG during relatively stable signal conditions (95.9 ± 4.0 vs. 95.3 ± 3.5%; p = 0.38, n = 11). The PZT sensor caused neither skin damage nor body movement increase in all neonates examined. ***Conclusion:*** The PZT sensor is noninvasive and does not cause skin irritation, and we believe it does provide a reliable, accurate cardiorespiratory monitoring tool for use in the NICU, although the issue of mechanical-ventilation noise remains to be solved.

Introduction

Cardiorespiratory monitoring of infants in the neonatal intensive care unit (NICU) is generally performed by electrocardiogram (ECG) and respiratory impedance pneumography (IPG), which utilizes ECG electrodes. These techniques are robust and widely used in the NICU

KARGER
Fax +41 61 306 12 34
E-Mail karger@karger.ch
www.karger.com

1661–7800/10/0982–0179$26.00/0

Accessible online at:
www.karger.com/neo

Shinichi Sato, PhD
Department of Cell Physiology, Akita University Graduate School of Medicine
1-1-1 Hondo
010-8543 Akita (Japan)
Tel. +81 18 884 6070, Fax +81 18 836 2604, E-Mail bigwave@gipc.akita-u.ac.jp

although the attachment of adhesive ECG electrodes is often difficult and is responsible for skin damage when it is used for very premature newborn infants or neonates after surgery [1]. In the pursuit of completely noninvasive cardiorespiratory monitoring, it is desirable for electrodes and sensors not to come into contact with the skin of a neonate. To solve this problem, other methods have been proposed to prevent skin damage at the site of ECG electrode attachment: a synthetic skin covering to protect the skin of low birth weight infants [1], a shirt incorporating a cardiorespiratory monitor [2] and a respiratory inductive plethysmography system that utilizes a belt-type sensor that requires passing no current through the neonate's body [3]. An electronic stethoscope [4] and echocardiography [5, 6] are also advanced methods which use no ECG electrodes to examine cardiac function, but their sensors still need to be in contact with the skin of a neonate and are unlikely to be suitable for cardiac monitoring over a long period. Recently, we developed a noninvasive cardiorespiratory-monitoring system for mice using a piezoelectric transducer (PZT) sensor (ATC-402; Unique Medical, Japan) [7–9], and based on this, we designed a PZT sensor for newborn infants (Pat. pending: PCT/JP2005/012068). As the PZT sensor is covered with a folded towel under the neonate, it never comes into contact with the skin (fig. 1). The PZT sensor passively detects acoustic vibrations produced by the heartbeats and breathing movements of a neonate and converts them into an electrical signal, from which the heart rate (HR) and breathing rate (BR) can be calculated. In the present study, we assessed the performance and feasibility of the new noninvasive PZT sensor for cardiorespiratory monitoring of newborn infants in the NICU by comparing with ECG and IPG.

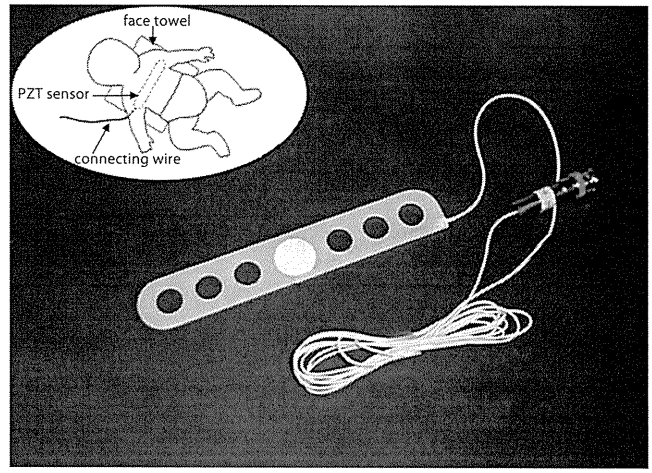

Fig. 1. PZT sensor. A round and thin PZT adheres to the lower side and center of a flexible plastic plate (width × depth × height, 180 × 30 × 1 mm) with several holes. The PZT sensor is put under a folded towel (~5 mm thick), on which a neonate is placed for cardiorespiratory monitoring, as illustrated in the inset. The PZT sensor was approved by the Ministry of Health, Labour and Welfare in Japan (No. 13B1X10014).

Methods

Subjects

Ethics approval for this project was granted by the Human Ethics Committee of Akita University School of Medicine. Seventy-nine neonates (50 boys and 29 girls) born at 25–42 (median 35) weeks of gestational age (GA) with birth weights (BWs) of 742–4,126 (median 2,140) g were recruited from the NICU, Akita University Hospital (table 1). Cardiorespiratory monitoring by PZT sensor was performed from June 2004 to January 2008 in 69 neonates, whose parents received oral information about the purpose of the study and gave written consent. Another 10 neonates underwent conventional ECG monitoring without the PZT sensor to assess if there is an adverse effect of the PZT sensor on neonates. Although 298 inpatients were eligible, only a small population was enrolled in the study because we had only one or two PZT sensor systems available for measurement during the period.

We carefully performed a preliminary study for 2 years from 2004 with 25 neonates to confirm the practical use of a PZT sensor for cardiorespiratory monitoring in the NICU and to determine the shape of the PZT sensor. Connections to a patient monitor to record ECG and IPG became available in June 2006 and May 2007, respectively. After the preliminary study and approval of the PZT sensor by the Ministry of Health, Labour and Welfare in Japan (approval No. 13B1X10014), we performed HR and BR measurements using the approved PZT sensor in 29 (from 2006) and 15 (from 2007) neonates, respectively, to evaluate the PZT sensor system. Six data were omitted from analysis: 2 poor quality data of unknown causes and 4 data obtained with misconnections to the A/D converter in HR and BR measurement, respectively. Finally, a total of 63 data (25 + 27 + 11) were used for the assessment of the PZT sensor.

PZT Sensor Construction

The preliminary study led to the conclusion that the PZT sensor should be as small as possible for a neonate to sleep comfortably with no accompanying irritation or discomfort; therefore, we designed a PZT sensor that consisted of a thin PZT (EE27A-39A; FDK, Japan) and flexible plastic plate (width × depth × height, 180 × 30 × 1 mm) with several holes, in the middle of which the PZT was adhered (fig. 1). The holes in the plastic plate may help to prevent skin damage (bedsores), enabling air ventilation and diffusing moisture produced by sweat through the towel (~5 mm thick) placed between the neonate and the PZT sensor. The plastic plate was designed to collect the vibrations of heartbeats and breathing movements from a wide area and therefore the PZT sensor allows slight displacement from the best monitoring position.